DMD Fast Forward. Published on September 17, 2020 as DOI: 10.1124/dmd.120.000086
This article has not been copyedited and formatted. The final version may differ from this version.

A two-tiered *in vitro* approach to de-risk drug candidates for potential bile salt export pump inhibition liabilities in drug discovery

Michael J. Hafey[1*]; Robert Houle[1]; Keith Q. Tanis[2]; Ian Knemeyer[1]; Jackie Shang[1**]; Qing Chen[1***]; Andreas Baudy[3]; James Monroe[3]; Frank D. Sistare[3]; and Raymond Evers[1**]

Departments of: [1]Pharmacokinetics, Pharmacodynamics & Drug Metabolism (PPDM), [2]Genetics and Pharmacogenomics, [3]Safety Assessment and Laboratory Animal Resources (SALAR), Merck & Co., Inc., Kenilworth, NJ, USA

*Corresponding author

Michael Hafey
Merck & Co., Inc.
PO Box 2000
Rahway, NJ
USA

** Current address: Janssen Pharmaceuticals, Johnson & Johnson, Springhouse, PA, USA

*** Current address: Vertex Pharmaceuticals, Boston, MA, USA

DMD Fast Forward. Published on September 17, 2020 as DOI: 10.1124/dmd.120.000086
This article has not been copyedited and formatted. The final version may differ from this version.

Running Title: *In vitro* approach to de-risk compounds for BSEP inhibition

Corresponding Author:
Michael J. Hafey
Merck & Co., Inc.
PO Box 2000
Rahway, NJ, USA
michael_hafey@merck.com

Number of text pages - 15
Number of tables - 2
Number of figures – 10
Number of references - 39

Word Count:
Abstract – 250
Introduction – 748
Discussion - 1698

Abbreviations:
Acyl-glucuronide (AG)

Alanine aminotransferase (ALT)

Aspartate aminotransferase (AST)

Bile Salt Export Pump (BSEP)

Biliary excretion index (BEI)

Cyclosporin A (CsA)

Drug induced liver injury (DILI)

Ethacrynic acid glutathione conjugate (EA-SG)

Estradiol-17β-D-glucuronide ($E_2$17βG)

Hanks' balanced salt solution (HBSS)

In vitro biliary clearance ($Cl_{biliary}$)

Maximal unbound concentration at the inlet of the human liver ($fu*I_{in,max}$)

Micropatterned co-culture (MPCC)

Multidrug Resistance Protein (MRP)

Organic Anion Transporting Polypeptide (OATP)

Phosphate buffered saline (PBS)

Sodium Taurocholate Co-transporting Polypeptide (NTCP)

Steady state C_{max} ($C_{max,ss}$)

Taurocholate (TCA)

DMD Fast Forward. Published on September 17, 2020 as DOI: 10.1124/dmd.120.000086
This article has not been copyedited and formatted. The final version may differ from this version.

Abstract

Hepatocellular accumulation of bile salts by inhibition of bile salt export pump (BSEP/*ABCB11*) may result in cholestasis and is one proposed mechanism of drug induced liver injury (DILI). To understand the relationship between BSEP inhibition and DILI, we evaluated 64 DILI positive and 57 DILI negative compounds in BSEP, multidrug resistance protein 2 (MRP2), MRP3, and MRP4 vesicular inhibition assays. An empirical cutoff (5 µM) for BSEP inhibition was established based on a relationship between BSEP IC_{50} values and the calculated maximal unbound concentration at the inlet of the human liver ($fu*I_{in,max}$, assay specificity = 98%). Including inhibition of MRP2-4 did not increase DILI predictivity. To further understand the potential to inhibit bile salt transport, a selected subset of 30 compounds were tested for inhibition of taurocholate (TCA) transport in a long-term human hepatocyte micropatterned co-culture (MPCC) system. The resulting IC_{50} for TCA *in vitro* biliary clearance ($Cl_{biliary}$) and biliary excretion index (BEI) in MPCCs were compared to the compound's $fu*I_{in,max}$ to assess potential risk for bile salt transport perturbation. The data show high specificity (89%). Nine out of 15 compounds showed an IC_{50} value in the BSEP vesicular assay of <5µM, but the BEI IC_{50} was greater than 10-fold the $fu*I_{in,max}$, suggesting that inhibition of BSEP *in vivo* is unlikely. The data indicate that although BSEP inhibition measured in membrane vesicles correlates with DILI risk, that measurement of this assay activity is insufficient. A two-tiered strategy incorporating MPCCs is presented to reduce BSEP inhibition potential and improve DILI risk.

Statement of Significance

This work describes a two-tiered *in vitro* approach to de-risk compounds for potential bile salt export pump inhibition liabilities in drug discovery utilizing membrane vesicles and a long-term human hepatocyte micropatterned co-culture system. Cutoffs to maximize specificity were established based on *in vitro* data from a set of 121 DILI positive and negative compounds and associated calculated maximal unbound concentration at the inlet of the human liver ($fu*I_{in,max}$) based on the highest clinical dose.

DMD Fast Forward. Published on September 17, 2020 as DOI: 10.1124/dmd.120.000086
This article has not been copyedited and formatted. The final version may differ from this version.

Introduction

Drug Induced Liver Injury (DILI) is the single most common adverse event leading to withdrawal of pharmaceuticals from the market and is a major reason for failure of drug candidates in development (Holt et al., 2010). Currently, DILI is difficult to predict with existing preclinical or *in vitro* models with only half of drugs that cause human hepatotoxicity being identified during preclinical testing (Sistare et al., 2016). Furthermore, the causes of DILI are likely multifactorial: as such, there is no single assay available to de-risk for DILI at the preclinical stage. Instead, a battery of assays is used with a 'weight of evidence' assessment (Shah et al., 2015). *In vitro* assays have been established to examine potential mechanisms including measurements of drug bioactivation, mitochondrial toxicity, and disruption of bile salt transport (Sistare et al., 2016, Wu et al., 2019, Monroe et al.,, 2020 and Kang et al., 2020).

Over the past decade, extensive research has been conducted to gain a better mechanistic understanding of disruption of bile salt transport and its relationship with DILI risk. The entero-hepatic circulation of bile salts is complex, with intestinal and hepatic membrane transporters playing a critical role in bile salt homeostasis (Yang et al., 2013). In humans, uptake of bile salts from the plasma into the hepatocyte is mediated by the sodium taurocholate co-transporting polypeptide (NTCP) and organic anion transporting polypeptide 1B1 and 1B3 (OATP1B1 and 1B3), while efflux of bile salts from the hepatocyte into the bile is mediated mainly by BSEP, the rate limiting step in bile salt transport, and to some extent by the multidrug resistance protein 2 (MRP2) (Yang et al., 2013, Figure 1).

BSEP-mediated efflux represents the driving force for the generation of bile salt dependent bile flow and thus, inhibition of BSEP may lead to elevations in intracellular bile salts in hepatocytes which can contribute to DILI (Kenna et al., 2018). Compensatory transport mechanisms, including down regulation of the sinusoidal uptake transporters (NTCP/OATP) and upregulation of both sinusoidal (MRP3, MRP4, OSTα/β) and canalicular efflux transporters (BSEP/MRP2), primarily through FXR signaling, aid in maintaining cellular bile salt homeostasis (Rodrigues et al., 2014).

To increase understanding of the relationship between BSEP inhibition and DILI, several groups have examined inhibition of BSEP-mediated transport of taurocholic acid (TCA) by drugs in a vesicular BSEP inhibition assay (Dawson et al., 2011, Morgan et al., 2010, Pedersen et al., 2013, Yucha et al., 2017). These studies show that several drugs implicated in DILI inhibit BSEP, but that there were false positives (i.e. BSEP inhibitors which were not DILI positive varied from 7 to 38%). IC_{50} cutoffs used to define BSEP inhibitors of concern varied widely, ranging from <25 μM (Morgan et al., 2010) to <300 μM (Dawson et

DMD Fast Forward. Published on September 17, 2020 as DOI: 10.1124/dmd.120.000086
This article has not been copyedited and formatted. The final version may differ from this version.

al., 2011). In addition, differences in compound test sets, adjudication of compounds as DILI positive, and *in vitro* inhibition values added additional complexity. False positives can also be due to the fact that membrane vesicles lack the metabolic and transport mechanisms needed to assess metabolites and/or interplay with other bile acid transporters in hepatocytes. Thus, further evaluation of compounds found to inhibit BSEP in vesicles is warranted in a hepatocyte-based model. Several groups have used sandwich cultured hepatocytes to assess drug effects on hepatobiliary bile acid disposition (Yang et al., 2016), but to our knowledge no comprehensive comparison has been conducted between DILI+ and DILI- compounds in both vesicles and a hepatocyte-based model.

Human hepatocyte micropatterned co-cultures (MPCC) are a bio-engineered microliver platform where human hepatocytes and mouse fibroblasts are plated in co-culture and in which stable expression of phase I and II enzymes and several transporters is maintained over several weeks in culture (Khetani and Bhatia, 2008). Furthermore, functional OATP, NTCP, and MRP2 activity has been shown (Khetani and Bhatia, 2008, Ramsden et al., 2013). Here, we explored whether MPCCs may serve as a platform to evaluate the effect of test compounds on bile salt transport and whether compounds which inhibit BSEP in membrane vesicles also inhibit canalicular efflux in MPCCs. Furthermore, we sought to understand the relationship between *in vitro* BSEP, MRP2, MRP3, and MRP4 inhibition, liver exposure, and human DILI risk prediction by examining the inhibition potential of 64 DILI positive and 57 DILI negative compounds on these transporters. For a subset of 30 compounds (19 DILI positive and 11 DILI negative), the inhibition of the uptake and efflux of TCA in MPCCs was evaluated to test the hypothesis that BSEP inhibition in vesicles results in a decreased BEI in MPCCs.

Methods

Materials

Membrane vesicles containing human BSEP, MRP2, MRP3, or MRP4 were manufactured by Genomembrane (Kanagawa, Japan) and purchased through Life Technologies (Grand Island, New York). [^{3}H]-TCA and [^{3}H]-estradiol-17β-D-glucuronide ($E_2$17βG) were purchased from Perkin Elmer. [^{3}H]-Folic Acid was purchased from Moravek, Inc. (Brea, California). [^{14}C]-ethacrynic acid glutathione conjugate (EA-SG) and all MK compounds included in this work were synthesized by Merck & Co., Inc. (Kenilworth, NJ, USA). Test compounds were purchased from a variety of commercial sources (as referenced in Monroe et al., currently in draft review). All other reagents were commercially obtained and were of the highest possible grade possible.

DMD Fast Forward. Published on September 17, 2020 as DOI: 10.1124/dmd.120.000086
This article has not been copyedited and formatted. The final version may differ from this version.

Classification of DILI positive and negative compounds

The list of drugs included in this study and their DILI positive or negative categorical assignments are provided in Table 1 as referenced in Monroe et al., currently in draft review. Several sources were referenced to make judgments on liver safety for drugs used for this assessment including clinical case reports from published literature, product labels, the NIH LiverTox database, and published country registries. Marketed drugs labeled with more moderate and non-life-threatening increases in aminotransferases representing a reversible and adaptive response to drug treatment, and not documented to be accompanied by acute liver failure as an indication of permanent injury to the liver, were not classified as DILI positive clinical hepatotoxicants. Market exposure over time as well as daily dose were also considered as drugs that are administered safely at relatively high doses resulting in significant daily liver dose burdens without liver injury support the classification of non-toxicants. True clinical hepatotoxicants were identified for testing among marketed or marketed but withdrawn compounds that have documented clinical diagnoses of acute liver failure. In addition, compounds were selected for inclusion in the test set that have been discontinued by pharmaceutical sponsors at clinical stages of drug development due to strong liver safety transaminase signals, but without allowing instances of acute liver failure. For such drugs, the liver safety signals were considered sufficiently strong for sponsors to discontinue development and so are representative of the type of test compounds that needs to be identified earlier, and therefore were also characterized as true clinical DILI positives in our analyses.

Inhibition of transport by BSEP, MRP2, MRP3 and MRP4 in membrane vesicles

The inhibitory effect of test compounds on ATP-dependent [^{3}H]TCA (1µM), [^{14}C]EA-SG (1µM), [^{3}H]$E_2$17BG (1µM), or [^{3}H]folic acid (10µM) uptake was conducted in membrane vesicles isolated from Sf9 cells containing BSEP, MRP2, MRP3, and MRP4 respectively, using 3 test compound concentrations (1 µM, 10 µM, and 25 µM) as described previously (Prueksaritanont et al., 2014). Transporter-mediated uptake was calculated by subtracting the uptake of the probe substrate in the presence of AMP from that in the presence of ATP. Data were normalized to % control, where uptake in the absence of test compound was 100%. Estimated IC_{50} values for inhibition of transporter-mediated uptake were obtained by fitting the data using equation 1 by nonlinear regression analysis using GraphPad Prism.

$$\text{Eq. 1: } \% \text{ Control} = 100/(1 + (\frac{I^{\text{Hill Slope}}}{IC50^{\text{Hill Slope}}}))$$

DMD Fast Forward. Published on September 17, 2020 as DOI: 10.1124/dmd.120.000086
This article has not been copyedited and formatted. The final version may differ from this version.

Where "control (%)" represents transporter-mediated uptake measured in the presence of various concentrations of inhibitor to that in the absence of inhibitor and "I" represents nominal inhibitor concentration (μM). Estimated IC_{50} values were extrapolated up to 100 μM. In instances when an estimated IC_{50} could not be estimated, the IC_{50} value was noted as >100 μM. To assess the accuracy of the three-point IC_{50} values, estimated IC_{50} values for 7 compounds including bosentan, nefazodone, and troglitazone were compared to literature values and found to be within three-fold of the published values (Dawson et al., 2012, Morgan et al., 2013).

The resulting IC_{50} values were compared to the estimated unbound concentration of test compounds at the inlet of the human liver ($fu*I_{in,max}$), which was calculated according to the approach described by Hirano et al. (2004) using the highest clinical dose prescribed or tested in the clinic, and corresponding published C_{max} values obtained from a variety of sources including PharmaPendium®, American Hospital Formulary Service (AHFS) Drug Information (http://www.ahfsdruginformation.com), and drug labels (Table 1). Empirical cutoffs were then established to limit the number of false positives and maximize assay specificity. Specifically, a threshold was set for BSEP, MRP2, MRP3, and MRP4 according to equations (Eq) 2-5, respectively:

$$Eq\ 2\text{: } (Log10(1/IC50) + 0.87) * (2 + Log10(Fu * Iin,max)) = 0.1$$

$$Eq\ 3\text{: } (Log10(1/IC50) + 1.9) * (2 + Log10(Fu * Iin,max)) = 0.1$$

$$Eq\ 4\text{: } (Log10(1/IC50) + 1.85) * (0.6 + Log10(Fu * Iin,max)) = 0.05$$

$$Eq\ 5\text{: } (Log10(1/IC50) + 1.6) * (2.2 + Log10(Fu * Iin,max)) = 0.5$$

Where values above 0.1 (BSEP and MRP2), 0.05 (MRP3), and 0.5 (MRP4) indicate that inhibition of the transporter may be indicative of DILI risk.

Fluorescent imaging of biliary canaliculi as well as BSEP and MRP2 localization in in human MPCCs

Human HepatoPac™ MPCCs plated in black-walled 96 well plates were purchased from Ascendance Bio (Medford, MA) and used for all imaging experiments. Live visualization of bile canaliculi was performed after incubation with 10 μM Carboxy-DCFDA 5-(and-6)-Carboxy-2',7'-Dichlorofluorescein Diacetate for 20 min at 37°C, followed by fluorescent imaging using an In Cell 2000 imager (GE Healthcare).

Immunostaining for BSEP and MRP2 was performed initially by fixation in 4% *para*-formaldehyde for 15 min. Wells were then washed two times with PBS before incubation with 1% Triton X100 for 10 min, 1%

DMD Fast Forward. Published on September 17, 2020 as DOI: 10.1124/dmd.120.000086
This article has not been copyedited and formatted. The final version may differ from this version.

BSA in PBS for 30 min at 37°C, and then with primary antibodies against BSEP (Santa Cruz N-16 #sc-17292; Jara et al 2009) and MRP2 (Millipore #MAB4148; Scheffer et al 2000) at 1:200 dilutions in PBS for 1 hr at 37°C. Wells were then washed four times with PBS and incubated for 1 hr at 37°C with Alexa Fluor 488 goat anti-rabbit IgG (Life Tech # A11034) and Alexa Fluor 647 goat anti-mouse IgG (Life Tech #A21236) at 1:500 in 0.1% Triton X100. Wells were then washed four times with PBS prior to fluorescent imaging using a GE In Cell 2000 Imager.

Inhibition of intrinsic in vitro biliary clearance and biliary excretion index in human MPCCs

The inhibitory effect of the test compound on the intrinsic *in vitro* biliary clearance ($Cl_{biliary}$) and biliary excretion index (BEI) of [^{3}H]TCA (1 µM) was conducted in human HepatoPac^{TM} MPCCs at Ascendance Bio (Medford, MA) using a similar method to that used in sandwich cultured hepatocytes described in Wolf et al.(2010).

Cryopreserved human hepatocytes (Celsis, Baltimore, MD) and cryopreserved 3T3 J2 mouse fibroblasts (stromal cells) were used to create MPCCs as described in Ukairo et al. (2013). Hepatocytes were from a single male human donor (Triangle Research Labs Lot GC4008) which was selected based on the uptake and efflux windows obtained with TCA after screening five hepatocyte lots. Culture medium was replaced every 2 days for 8 days. All reagents used in the study were of analytical grade.

The transport of [^{3}H]TCA was measured in 96-well human MPCCs in the presence and absence of varying concentrations of test compound or cyclosporin A (CsA, positive control for transporter inhibition) after 10 min or 24 hr preincubation with test compound. Twenty-four hr preincubations were carried out in hepatocyte culture medium without serum. Ten minutes prior to initiation of uptake/efflux assays, cells were washed three times in Hanks' Balanced Salt Solution (HBSS) buffer containing calcium or HBSS devoid of calcium before incubation with buffers containing test compounds. MPCCs used to measure TCA uptake into the hepatocytes and efflux into the canalicular space were incubated in buffer containing calcium, whereas cells used to measure uptake into hepatocytes were incubated in buffer devoid of calcium for 10 min at 37°C (Wolf et al, 2010). All wells were then washed with HBSS containing calcium. Transport was initiated by the addition of TCA (1 µM; 0.5 µCi/ml) in the presence or absence of various concentrations of test compound or CsA in HBSS containing calcium at 37°C for 10 min for uptake and efflux assessments. Transport was stopped by the addition of ice-cold phosphate buffered saline (PBS), cells were washed three times in ice-cold PBS, and lysed (1% Triton X100 in PBS) for 20 mins. Cell lysates were pipetted up and down several times and then transferred to scintillation

DMD Fast Forward. Published on September 17, 2020 as DOI: 10.1124/dmd.120.000086
This article has not been copyedited and formatted. The final version may differ from this version.

vials or plates containing scintillation fluid. The radioactivity of each sample was measured using liquid scintillation counting. All compounds were analyzed in triplicate.

Protein was extracted from representative MPCC wells by lysing the cells in RIPA buffer (Rockland Immunochemicals Inc., Gilbertsville, PA) for 5 min on ice. The amount of protein per well was measured using the Pierce BCA Protein Assay kit (Rockford, IL). The protein content of stromal only cultures was also measured, and hepatic protein was calculated by subtracting stromal only protein from MPCC protein values. The scintillation counts were then normalized by hepatic protein content. The experiment was performed in triplicate.

The $Cl_{biliary}$ and BEI were calculated using the mean scintillation counts in equations 6 and 7 (Wolf et al, 2010):

$$\text{Eq 6: } \text{in vitro } Cl_{biliary} = \frac{\text{accumulation}_{cells+bile} - \text{accumulation}_{cells}}{AUC_{medium}}$$

$$\text{Eq 7: } BEI = \frac{\text{accumulation}_{cells+bile} - \text{accumulation}_{cells}}{\text{accumulation}_{cells+bile}} \text{x}100$$

where accumulation in cells plus bile was determined in MPCCs preincubated in HBSS containing calcium and cellular accumulation of substrate in cells alone was determined in MPCCs preincubated in HBSS buffer devoid of calcium. The AUC_{medium} was defined to be a constant (equal to 1) as the concentration of TCA in the incubation media was not expected to change over the course of the experiment (Wolf et al., 2010).

TCA transport was calculated by subtracting the accumulation in stromal cell only cultures from the accumulation in MPCCs. The data were normalized to % control, where $Cl_{biliary}$ or BEI in the absence of test compound was defined as 100%. IC_{50} values were obtained by fitting the data using equation 8 by nonlinear regression analysis using GraphPad Prism.

$$\text{Eq. 8: Control (\%)} = 100 / ((1+I)/IC_{50})$$

Where “control (%)” represents transporter-mediated uptake/efflux measured in the presence of various concentrations of inhibitor to that in the absence of inhibitor and “I” represents the nominal inhibitor concentration. Compounds were tested up to 25 or 50 µM based on solubility limitations. IC_{50}

DMD Fast Forward. Published on September 17, 2020 as DOI: 10.1124/dmd.120.000086
This article has not been copyedited and formatted. The final version may differ from this version.

values were not extrapolated beyond the top test concentration. Data are expressed as mean ± SE where SE describes the standard error of the curve fit.

Metabolite Identification in MPCCs

Following a 24 hr pre-incubation of test compound in serum free hepatocyte media with MPCCs, acetonitrile containing 0.1% formic acid was added to the wells to bring the organic concentration to 75%. Wells were thoroughly mixed and cell lysate and media were collected in 96 well plates. Plates were then spun at 3000 x g for 5 min to precipitate cellular proteins. Supernatant was collected from each well and pooled with n = 3 replicates to increase metabolite amounts. The metabolite identification was performed using a Xevo G2 Q-TOF high resolution mass spectrometer (Waters Corp., Milford, MA, USA) equipped with an electrospray source operated in positive mode and coupled with an Acquity UPLC system (Waters Corp., Milford, MA, USA). Chromatographic separation for metabolite identification was achieved on a Kinetex C18 column (2.6 u, 100 mm x 2.1 mm I. D., Phenomenex , Torrance, CA, USA). The gradient elution was started from 5% B and increased to 80% B linearly in 10 min, then maintained for 2 min, finally decreased to 5% B to equilibrate the column. The flow rate was set at 0.5 mL/min, and the column temperature was maintained at 40 °C. High resolution MS and MS/MS acquisitions parameters were set as follows: source temperature, 150 °C; desolvation temperature, 350 °C; cone voltage, 35 V. Data were acquired from 80−1300 Da. The mass spectrometer and UPLC system were operated with MassLynx 4.1 software. The metabolite data processes were done by Metabolynx XS.

Results

Development of BSEP and MRP2-4 inhibition vesicular screening assays

Inhibition assays were established to examine the effect of test compound on human BSEP, MRP2, MRP3, and MRP4-mediated transport in membrane vesicles isolated from baculovirus infected Sf9 cells containing the transporter of interest. Uptake of probe substrates increased 7.6, 6.3, 3.8, and 3.1-fold in the presence of ATP compared to that observed in the absence of ATP for BSEP, MRP2, MRP3, and MRP4 assays, respectively (Figure 2A-D). ATP-dependent uptake was abolished by the inhibitors atorvastatin (BSEP) and bromosulphophthalein (MRP2, MRP3, and MRP4), confirming the functionality of the assays. Of note, TCA was not used as the probe substrate in MRP2-4 inhibition assays, because assay windows were < 2-fold (data not shown).

DMD Fast Forward. Published on September 17, 2020 as DOI: 10.1124/dmd.120.000086
This article has not been copyedited and formatted. The final version may differ from this version.

Establishment of an empirical vesicular BSEP assay cutoff based on the relationship between BSEP IC_{50} and liver fu$I_{in,max}$*

To evaluate the relationship between *in vitro* BSEP inhibition in membrane vesicles and human DILI risk, the inhibitory effect of 64 DILI positive and 57 DILI negative compounds on ATP-dependent [^{3}H]TCA uptake was measured. The resulting estimated BSEP IC_{50} values were compared to the compound's fu*$I_{in,max}$ (Table 1), which was estimated according to the approach described by Hirano et al. (2006) using the highest clinical dose prescribed to patients and corresponding C_{max} values (Figure 3). An empirical cutoff was then established to limit the number of false positives and to maximize assay specificity. Inhibition of BSEP was predictive of human DILI for compounds that fell above the empirical cutoff, while inhibition of BSEP was not predictive of human DILI for compounds below the cutoff. The specificity of the assay was high (98%, Figure 3B) with only one false positive (dipyridamole) identified. Sensitivity was low (23%) as anticipated, most likely because DILI for these compounds was caused by mechanisms other than BSEP inhibition. In the absence of dose and exposure data to calculate fu*$I_{in,max}$, a cutoff of 5 µM could be set because, based on a sensitivity analysis, 5 µM yielded similar results as the empirical cutoff with one additional false positive (rosiglitazone) identified (Figure 3C).

Contribution of inhibition of MRP2-4 in addition to BSEP to predictivity of DILI risk

To assess whether inhibition of human MRP2, MRP3, and MRP4 would increase the predictivity of human DILI risk, the inhibitory effect of the DILI test set on ATP-dependent uptake of probe substrates was measured in membrane vesicles (Table 1). The results in Figure 4 indicated that: 1) A compound positive for BSEP inhibition *(i.e.* IC_{50} value below the empirical cutoff), regardless of inhibition of MRP2-4, may have an increased DILI risk; 2) Inhibition of MRP2-4 alone lowered the positive predictive value of the assay as compared to BSEP alone because it increased the number of false positives (Figure 4A, left panel, Figure 4B); and 3) MRP2-4 inhibition in addition to inhibition of BSEP decreased the overall specificity of DILI predictions, because it increased the number of false positives (Figure 4B).

MPCC's are a functional hepatocyte-based system to evaluate inhibition of bile salt efflux

To investigate whether inhibition of BSEP in membrane vesicles correlated with a decrease in the canalicular efflux of TCA in human hepatocytes, MPCCs were explored. Characterization studies were first conducted to determine the localization and activity of BSEP in MPCCs. Figure 5 shows the presence of bile canaliculi as well as the canalicular localization of MRP2 and BSEP by measuring CDF (5-carboxy-2', 7' dichlorofluorescein) accumulation in the canalicular space (panel A) and the immunolocalization of

DMD Fast Forward. Published on September 17, 2020 as DOI: 10.1124/dmd.120.000086
This article has not been copyedited and formatted. The final version may differ from this version.

MRP2 and BSEP using specific antibodies (panel B), respectively. CDF accumulation in the canalicular space also demonstrated functional MRP2 efflux as MRP2-mediated efflux of CDF has been shown previously (Zamek-Gliszczynski et al., 2003). Functional activity of BSEP was demonstrated by the time dependent accumulation of [^{3}H]TCA in the presence of calcium (Figure 6A). This accumulation represents total accumulation of TCA in both the hepatocyte and the bile canalicular space (Wolf et al., 2010), and thus is the sum of sinusoidal uptake and sinusoidal and canalicular efflux. By preincubating co-cultures in buffer with or without calcium to modulate cellular tight junctions, distinguishing between TCA accumulation in cellular and bile canalicular compartments was possible (Figure 6B). This methodology enables the calculation of $Cl_{biliary}$ and BEI (reviewed by Brouwer et al., 2013, Swift et al., 2010 and Yang et al., 2016). The $Cl_{biliary}$ represents the net effect of uptake of TCA across the sinusoidal membrane into the hepatocyte as well as its efflux across the canalicular membrane into the bile canaliculi. The BEI represents the percent of TCA accumulation that resides in the bile canaliculi (i.e. efflux across the canalicular membrane) and was >50% for control incubations in all studies. Inhibition of $Cl_{biliary}$ with no change in BEI indicates that the uptake of TCA is inhibited by the test compound and canalicular efflux of TCA is not, while inhibition of both $Cl_{biliary}$ and BEI suggests that canalicular efflux of TCA is inhibited with or without concurrent uptake inhibition (Wolf et al., 2010). Cyclosporin A (CsA), a known NTCP, OATP1B and BSEP inhibitor (Mita, 2006, Yoshida, 2012), inhibited the $CL_{biliary}$ and BEI of TCA after a 10 min and 24 hr preincubation (Figure 7A-C, 24 hr data not shown). The resulting IC_{50} values for CsA inhibition of $CL_{biliary}$ of TCA after a 10 min or 24 hr preincubation were 2.4 ± 0.8 and 1.1 ± 0.2 µM, respectively. The resulting IC_{50} values for CsA inhibition of BEI of TCA after a 10 min or 24 hr preincubation were 4.7 ± 1.3 and 2.2 ± 0.4 µM, respectively, indicating that both sinusoidal uptake and canalicular efflux were inhibited. While a 10 min preincubation with test compound is commonly used (Kenna et al., 2018), a 24 hour preincubation timepoint was included in all studies to allow for potential metabolite effects on BEI to be observed as metabolite formation will be low for the majority of compounds following a 10 minute incubation. In the case of cyclosporin A, parent accounted for ~95% of total compound found in the incubation after 24 hr, while the remaining ~5% consisted of two oxidative metabolites and one metabolite formed from demethylation (supplemental data). Taken together, these data indicated that MPCCs are a functional hepatocyte co-culture system to examine the effects of test compounds on the uptake and efflux of TCA.

Correlation between inhibition of BSEP in membrane vesicles and inhibition of BEI in MPCCs

DMD Fast Forward. Published on September 17, 2020 as DOI: 10.1124/dmd.120.000086
This article has not been copyedited and formatted. The final version may differ from this version.

The effect of 19 DILI positive and 11 DILI negative compounds on the uptake and efflux of TCA was measured in human MPCCs. The compound set was chosen without bias from the 121 compounds test in membrane vesicles and included both BSEP inhibitors and non-inhibitors. The resulting IC_{50} values for TCA $Cl_{biliary}$ and BEI were compared to the $fu*I_{in,max}$ for each compound (Table 2). When the IC_{50} value was ≤ 10-fold the $fu*I_{in,max}$, a static cutoff used to assess DDI risk for cytochrome P450 enzymes (FDA draft guidance, 2017), compounds were classified as having a risk to inhibit sinusoidal uptake or both sinusoidal uptake and canalicular efflux in humans. To determine whether BSEP inhibition measured in membrane vesicles correlated with a decrease in TCA canalicular efflux (*i.e.* a decrease in BEI of TCA) in MPCCs, the IC_{50} for BEI of TCA after a 24 hr preincubation was compared to the $fu*I_{in,max}$ for all compounds tested (Figure 8A). Nine out of 15 compounds which showed an IC_{50} value in the BSEP vesicular inhibition assay of < 5 µM did not demonstrate an IC_{50} for BEI that was less than 10-fold the $fu*I_{in,max,}$ (Figure 8B), suggesting that BSEP inhibition in humans would be unlikely at clinically relevant exposures. A sensitivity analysis (Figure 8C) showed that the specificity of the MPCC assay to predict DILI positive compounds using the calculated BEI in conjunction with the $fu*I_{in,max}$ was high (89%) with only one false positive (lopinavir) identified. Interpretation of the false positive is confounded by the fact that lopinavir is co-administered with ritonavir as a PK enhancer in the form of Kaletra and some degree of serum aminotransferase elevations occur in a high proportion of patients taking lopinavir containing antiretroviral regimens (livertox.nih.gov).

Case Study: Effect of the GPR40 Agonist MK-8666 on Bile Salt Transport Inhibition

MK-8666, a small molecule agonist of the GPR40 receptor that was in development for the treatment of type 2 diabetes mellitus (Hyde, 2016), was terminated due to concerns about its liver safety. As detailed in Shang et al. (2019), "a 53-year-old male subject in the 150-mg QD cohort demonstrated increases in alanine aminotransferase (ALT) and aspartate aminotransferase (AST) above baseline prior to dosing on day 3 and showed an upward trend on continued dosing. The highest observed ALT and AST values were measured 24 h after the final dose of MK-8666 (4−5× and 2−3× upper-limit-of-normal, respectively), along with concurrent elevation in alkaline phosphatase (1.4× upper-limit-of-normal). These findings reversed within 2 weeks after the completion of dosing to normal or near-normal concentrations. Our company terminated the clinical development of MK-8666 in anticipation of an unfavorable benefit/risk profile" (Krug, 2017).

To assess whether inhibition of BSEP could contribute to the liver toxicity observed for MK-8666, the IC_{50} for BSEP was measured in membrane vesicles: the IC_{50} was found to be 0.8 ± 0.08 µM (Figure 9A), which

DMD Fast Forward. Published on September 17, 2020 as DOI: 10.1124/dmd.120.000086
This article has not been copyedited and formatted. The final version may differ from this version.

was above the empirical cutoff established in Figure 3 (Panel A). Subsequently, the inhibition of the uptake and efflux of TCA by MK-8666 in MPCCs was determined. After a 24 hr pre-incubation, MK-8666 inhibited the $Cl_{biliary}$ of TCA with an IC_{50} of 23.6 ± 10.5 µM (data not shown). At 25 and 50 µM, the highest concentrations tested, MK-8666 inhibited ~ 31 and 97% of the BEI of [^{3}H]TCA, respectively, resulting in an IC_{50} of > 25 µM (Figure 9B). The IC_{50} values were >10-fold the calculated fu*$I_{in,max}$ even at a dose of 500 mg.

To explore whether metabolism of MK-8666 in MPCCs explains the discrepancy between potency in the vesicular and MPCC inhibition assays, the metabolism of MK-8666 was examined. After a 24 hr incubation, approximately 80% of MK-8666 was converted to an acyl-glucuronide (AG) metabolite (Figure 9C). Follow-up studies in BSEP membrane vesicles showed that the MK-8666-AG was not an inhibitor of BSEP-mediated [^{3}H]TCA uptake (IC_{50} > 25 µM) (Figure 9D).

Discussion

In this study, we sought to understand the relationship between *in vitro* BSEP inhibition measured in membrane vesicles and human DILI risk by examining the inhibition potential of 121 DILI positive or negative compounds. Through the establishment of an empirical cutoff designed to maximize assay specificity, a relationship was established between vesicular BSEP inhibition and DILI risk by comparing BSEP inhibition potency to the calculated fu*$I_{in,max}$. While inhibition of BSEP in the vesicular inhibition assay may be predictive of DILI risk for compounds above the empirical cutoff, causality has not been demonstrated.

While membrane vesicles can be used as a first step to assess BSEP inhibition, they lack metabolic activity and capture only one factor involved in bile acid disposition (Kenna et al., 2018). As such, false positives and negatives would be expected based on the vesicle assay alone. MPCCs, in contrast, allow for a more holistic assessment of bile salt transport inhibition as multiple transport and metabolic pathways are active (Khetani and Bhatia, 2008, Ramsden et al., 2013, Moore et al., 2016, Kratochwil et al., 2018). To test the hypothesis that BSEP inhibition in vesicles results in decreased BEI in MPCCs, studies with a subset of compounds were conducted in MPCCs to assess the inhibition of both uptake and efflux of TCA.

Inhibition of BSEP in vesicles was not predictive of inhibition of canalicular efflux of TCA in MPCCs for some compounds including the anti-thrombotic dipyridamole, the false positive in the vesicular analysis (Figure 3A and 8B). Overall, the data show that there is no correlation between the IC_{50} values generated

DMD Fast Forward. Published on September 17, 2020 as DOI: 10.1124/dmd.120.000086
This article has not been copyedited and formatted. The final version may differ from this version.

in the two assays (Table 2). Approximately 13% of the 121 compounds tested in the vesicular inhibition test set warranted further evaluation in MPCCs based on the cutoff of 5 µM. Of those tested in MPCC's, 33% were found to have the potential to inhibit canalicular efflux of bile salts in vivo. As an example, metabolism of dipyridamole in MPCCs likely explains the discrepancy between potency in the vesicular and MPCC inhibition assays as dipyridamole was completely converted to an AG metabolite in the incubation (supplemental data). In addition to metabolism, discrepancies between inhibition observed in vesicles and MPCCs may be explained by protein binding, intracellular sequestration, and/or compensatory mechanisms such as potential activation of various (nuclear) hormone receptors. Thus, caution is warranted in the interpretation of vesicular inhibition data alone. Importantly, our analysis in MPCCs does not consider the type of DILI associated with a compound, but rather focuses on potential to inhibit biliary efflux. Since inhibition of biliary efflux is only one potential mechanism causing/correlating with cholestatic liver injury (Balistreri et al., 2005, Burbank et al., 2016, Deferm et al., 2019), compounds known to be cholestatic in humans such as troglitazone, nefazodone, and bosentan may or may not be flagged using a 10-fold cutoff between the TCA BEI IC_{50} and $fu*I_{in,max}$ indicating altered transporter-mediated efflux.

Several others have examined the relationship between *in vitro* BSEP inhibition and prediction of human DILI risk (Morgan et al., 2011 and 2013, Dawson et al., 2011, Pendersen et al., 2013, Wolf et al., 2010, Yucha et al., 2017). While these studies have linked BSEP inhibition to DILI risk, most relationships have been built on BSEP potency alone or comparisons of BSEP potency and total (bound plus unbound) drug concentrations. However, based on the free drug hypothesis, correlations between total drug exposure and BSEP inhibition are unlikely to be causal. The most relevant exposure parameter to compare BSEP potency to is the unbound intrahepatic concentration of the drug. As this is difficult to measure *in vivo* (Guo et al., 2018), we compared BSEP potency to $fu*I_{in,max}$. This value can serve as a surrogate for unbound intracellular levels for non-transporter substrates as unbound plasma and tissue concentrations should be in equilibrium at steady state. Of note, most compounds showing discrepancies between assays were not known to be substrates for uptake transporters.

In a recently published whitepaper, the evaluation of BSEP inhibition was recommended in drug discovery and development to aid in DILI risk assessment (Kenna et al., 2018). A proposed guided workflow included initial screening in membrane vesicles and utilization of a 25 µM static cutoff followed by comparison of the BSEP IC_{50} to total steady state C_{max} ($C_{max,ss}$). In this analysis, a margin < 10 (*i.e.* BSEP IC_{50} < 10 fold total $C_{max,ss}$) was proposed to suggest a potential risk based largely on the data

DMD Fast Forward. Published on September 17, 2020 as DOI: 10.1124/dmd.120.000086
This article has not been copyedited and formatted. The final version may differ from this version.

published by Morgan et al. (2010). In the present study, this cutoff resulted in an increased rate of false positives (data not shown). Our BSEP vesicular analysis offers improvement to previous analyses as the use of $fu*I_{in,max}$ is a more relevant exposure parameter which increases assay specificity. In addition, our analysis also suggests the use of 5 µM as a static cutoff when dose and C_{max} predictions are not available allowing for early assessment of risk in drug discovery. It should be noted that the results are dependent on the selected test set and the extent to which the test set is representative for the current chemical space explored in medicinal chemistry.

For compounds identified as potential BSEP inhibitors in vesicles (*i.e.* BSEP IC_{50} < 10-fold total $C_{max,ss}$), the guided workflow in the whitepaper recommends undertaking investigatory studies which may include assessment of the BEI of TCA in a hepatocyte-based system such as sandwich cultured hepatocytes. Our data indicate that MPCCs can also be used as a functional hepatocyte-based system in which to evaluate potential to inhibit canalicular efflux of bile salts and support the need for hepatocyte-based models to overcome limitations of the vesicular inhibition assay alone. In addition, MPCCs have been shown to improve IVIVC by detecting primary and secondary metabolites (DaSilva et al., 2018).

Beyond the use of a hepatocyte-based model to evaluate inhibition of TCA efflux, the guided workflow suggests consideration of inhibition of other bile acid transporters including MRPs. MRP-mediated efflux has been proposed as a compensatory pathway used by hepatocytes to efflux accumulated intracellular bile salts into the plasma when BSEP is inhibited (Kock and Brouwer, 2012). The results in Figure 4 show that inhibition of MRP2-4 do not increase specificity of DILI predictions beyond BSEP inhibition alone and exhibit lower positive predictive value. Previous reports lacked alignment on the value of MRP inhibition in DILI risk assessment (Morgan et al., 2013, Kock et al., 2013, Yucha et al., 2017). One caveat to the MRP analyses is that probe substrates used in the MRP inhibition studies were not bile acids and we cannot exclude potential differences in inhibition profiles due to substrate-dependent inhibition. It is not unexpected that inhibition of MRPs, in the absence of BSEP inhibition, does not correlate with DILI risk as canalicular efflux via BSEP is the rate determining step in bile salt excretion. Furthermore, although clinical liver injury data is lacking for patients with polymorphic variants of MRP3/4, patients with polymorphic MRP2 resulting in complete loss of function (Dubin Johnson syndrome) do not exhibit increased incidence of liver injury (Kullak-Ublick et al., 2004). While inhibition of BSEP and MRPs could result in increases in intracellular concentrations of bile acids due to inhibition of both canalicular and sinusoidal efflux pathways, Ostα/β may provide an additional efflux pathway to lower concentrations inside hepatocytes (Ballatori et al., 2005, Li et al., 2007, Zhang et al., 2017).

DMD Fast Forward. Published on September 17, 2020 as DOI: 10.1124/dmd.120.000086
This article has not been copyedited and formatted. The final version may differ from this version.

Taken together, our data support a two-tiered approach to limit compounds with potential BSEP inhibition liabilities to enter clinical development (Figure 10). Early screening can be completed in membrane vesicles. In instances where a compound's IC_{50} is above the empirical cutoff established, assessment of TCA BEI inhibition potential can be conducted in MPCCs to further explore whether BSEP inhibition is of significance *in vivo*. Proactive use of this paradigm at Merck has allowed us to further de-risk vesicular BSEP inhibition results with MPCCs for several internal programs resulting in no known instances of clinical BSEP inhibition as exemplified by the MK-8666 case study. While initial inhibition studies with MK-8666 in membrane vesicles warranted further experimentation in MPCCs, the TCA BEI IC_{50} was greater than 10-fold the predicted $fu*I_{in,max}$. Because 80% of MK-8666 was metabolized to an AG in MPCCs and the AG did not inhibit BSEP in the BSEP vesicular assay, metabolism of MK-8666 was a likely cause for the lack of inhibition of TCA transport in the MPCCs. Supporting this finding, plasma samples from healthy volunteers exhibited no elevation in plasma levels of GCDCA on day 1 and 10 after receiving 800 mg QD of MK-8666 compared to those receiving placebo (data on file). A recent publication by Shang et al. (2019) suggests that an alternative mechanism could contribute to DILI risk for MK-8666: metabolism of the carboxylic moiety forms a reactive intermediate which covalently modifies proteins.

In instances where the TCA BEI IC_{50} in MPCCs is < 10 fold the $fu*I_{in,max}$, the test compound may have potential to inhibit BSEP *in vivo*. Given the lack of a specific biomarker and a translational pre-clinical model, one could develop structure–activity relationships (SAR) to screen out the liability *in vitro* or power a phase I study to include markers of cholestasis to assess toxicity potential early in humans. There are several caveats of this tiered approach. First, only compounds that are above the empirical cutoff in vesicles would be tested in MPCCs. Therefore, compounds forming a BSEP inhibiting metabolite, such as in the case of troglitazone sulfate (Funk et al., 2001), would be missed. Second, parameters used in the $fu*I_{in,max}$ calculation assume worst case scenario (i.e. Fa = 1, Ka = 0.1 min^{-1}). When available, measured values should be incorporated into the calculation to enhance the accuracy of the assessment. Third, due to compensatory mechanisms not all BSEP inhibitors will result in cholestasis. By eliminating compounds based on BSEP inhibition alone, one could halt development of a compound that may not present as cholestatic clinically. In the future, development of a relevant *in vivo* model that replicates drug induced BSEP inhibition to assess human DILI as well as leveraging *in vitro* / *in vivo* models to identify, qualify, and optimize the utility of translational biomarkers for BSEP inhibition for clinical application would be needed to further enhance a de-risking strategy.

Acknowledgements

We thank Amanda Moore and Okey Ukairo formerly of Ascendance Bio (Medford, MA) for technical support and scientific insight into this work. We thank Sheri Smith, Richard Gundersdorf, and Yuexia Liang for MPCC metabolite identification support.

Authorship Contributions

Participated in research design: Hafey, Houle, Sistare, and Evers

Conducted experiments: Hafey, Houle, Shang, Chen, and Baudy

Performed data analysis: Hafey, Houle, Tanis, Knemeyer, Shang, Chen, Baudy, and Monroe

Wrote or contributed to the writing of the manuscript: Hafey, Houle, Tanis, Baudy, Monroe, Sistare, and Evers

References

Ballatori, N., Christian, W.V., Lee, J.Y., Dawson, P.A., Soroka, C.J., Boyer, J.L., Madejczyk, M.S., and N. Li. (2005). OSTα-OSTβ: a major basolateral bile acid and steroid transporter in human intestinal, renal, and biliary epithelia. Hepatology 42, 1270-1279.

Brouwer K., Keppler. D, Hoffmaster, K., Bow, D., Cheng, Y., Lai, Y., Palm, J., Stieger, B., and R. Evers. (2013). In vitro methods to support transporter evaluation in drug discovery and development. Clin Pharmacol Ther. 94:95-112.

Burbank, M., Burban, A., Sharanek, A., Weaver, R., Guguen-Guillouzo, C., and A. Guillouzo. Early Alterations of Bile Canaliculi Dynamics and the Rho Kinase/Myosin Light Chain Kinase Pathway Are Characteristics of Drug-Induced Intrahepatic Cholestasis. Drug Metab Dispos. 44:1780-1793.

Da-Silva, F., Boulenc, X., Vermet, H., Compigne, P., Gerbal-Chaloin, S., Daujat-Chavanieu, M., Klieber, S., and P. Poulin. (2018). Improving prediction of metabolic clearance using quantitative extrapolation of results obtained from human hepatic micropatterned cocultures model and by considering the impact of albumin binding. J Pharm Sci. 107(7):1957-1972.

Dawson, S., Stahl, S., Paul, N., Barber, J., and J.G. Kenna. (2011). In vitro inhibition of the bile salt export pump correlates with risk of cholestatic drug-induced liver injury in humans. Drug Metab Dispos. 40, 130-138.

Deferm, N., De Vocht, T., Qi, B., Van Brantegem, P., Gijbels, E., Vinken, M., de Witte, P., Bouillon, T., and P. Annaert. (2019). Current insights in the complexities underlying drug-induced cholestasis. Crit Rev Toxicol. 49:520-548.

Funk C., Pantze, M., Jehle, L., Ponelle, C., Scheuermann, G., Lazendic, M., and R. Gasser. (2001). Troglitazone-induced intrahepatic cholestasis by an interference with the hepatobiliary export of bile acids in male and female rats. Correlation with the gender difference in troglitazone sulfate formation and the inhibition of the canalicular bile salt export pump (Bsep) by troglitazone and troglitazone sulfate. Toxicology. 167:83-98.

Guo, Y., Chu, X., Parrott, N., Brouwer, K., Hsu, V., Nagar, S., Matsson, P., Sharma, P., Snoeys, J., Sugiyama, Y., Tatosian, D., Unadkat, J., Huang, S., and A. Galetin. (2018). Advancing Predictions of Tissue and Intracellular Drug Concentrations Using In Vitro, Imaging and Physiologically Based Pharmacokinetic Modeling Approaches. Clin Pharmacol Ther. 104:865-889.

Hirano M, Maeda K, Shitara Y, Sugiyama Y. (2006). Drug-drug interaction between pitavastatin and various drugs via OATP1B1. Drug Metab Dispos. 34, 1229-123.

Hyde, A. M., Liu, Z., Kosjek, B., Tan, L., Klapars, A., Ashley, E.R., Zhong, Y.L., Alvizo, O., Agard, N.J., Liu, G., Gu, X., Yasuda, N., Limanto, J., Huffman, M.A., and D. M. Tschaen. 2016. Synthesis of the GPR40 Partial Agonist MK-8666 through a Kinetically Controlled Dynamic Enzymatic Ketone Reduction. Org Lett. 18, 5888-5891.

Itoh, Y., Kawamata, Y., Harada, M., Kobayashi, M., Fujii, R., Fukusumi, S., Ogi, K., Hosoya, M., Tanaka, Y., Uejima, H., Tanaka, H., Maruyama, M., Satah, R., Okubo, S., Kizawa, H., Komatsu, H., Matsumura, F., Moguchi, Y., Shinohara, T., Hinuma, S., Fujisawa, Y., and M. Fujino. (2003). Free fatty acids regulate insulin secretion from pancreatic cells through GPR40. Nature. 422, 173-176.

Kaimal, R., Song, X., Yan, B., King, R., and R. Deng. (2009). Differential modulation of farnesoid X receptor signaling pathway by the thiazolidinediones. J Pharmacol Exp Ther. 330:125-34.

Kang, W., Podtelezhnikov, A., Tanis, K., Pacchione, S., Su, M., Bleicher, K., Wang, Z., Laws, G., Griffiths, T., Kuhls, M., Chen, Q., Knemeyer, I., Marsh, D., Mitra, K., Lebron, J., and F. Sistare. (2020). Development and Application of a Transcriptomic Signature of Bioactivation in an Advanced In Vitro Liver Model to Reduce Drug-induced Liver Injury Risk Early in the Pharmaceutical Pipeline. Toxicol Sci. Online ahead of print.

Kenna, J., Taskar, K., Battista, C., Bourdet, D., Brouwer, K., Brouwer, K., Dai, D., Funk, C., Hafey, M., Lai, Y., Maher, J., Pak, Y., Pedersen, J., Polli, J., Rodrigues, A., Watkins, P., Yang, K., Yucha, R. on behalf of the International Transporter Consortium. (2018). Can Bile Salt Export Pump Inhibition Testing in Drug Discovery and Development Reduce Liver Injury Risk? An International Transporter Consortium Perspective. Clin Pharmacol Ther. 104:916-932.

Khetani S.R., and S.N. Bhatia. (2008). Microscale culture of human liver cells for drug development. Nat Biotechnol. 26, 120-126.

Kock, K., Ferslew, B., Netterberg, I., Yang, K., Urban, T., Swaan, P., Stewart, P., and K. Brouwer. (2014). Risk factors for the development of cholestatic drug induced liver injury: Inhibition of hepatic basolateral bile acid transporters multidrug resistance associated proteins 3 and 4. Drug Metabolism and Disposition. 42, 665-674.

Kock, K. and K.L. Brouwer. (2012) A perspective on efflux transport proteins in the liver. Clin Pharmacol Ther. 92, 599-612.

Kratochwil, N., Triyatni, M., Mueller, M., Klammers, F., Leonard, B., Turley, D., Schmaler, J., Ekiciler, A., Molitor, B., Walter, I., Gonsard, P., Tournillac, C., Durrwell, A., Marschmann, M., Jones, R., Ullah, M., Boess, F., Ottaviani, G., Jin, Y., Parrott, N., and S. Fowler. (2018). Simultaneous Assessment of Clearance, Metabolism, Induction, and Drug-Drug Interaction Potential Using a Long-Term In Vitro Liver Model for a Novel Hepatitis B Virus Inhibitor. J Pharmacol Exp Ther. 365:237-248.

Krug, A. W., Vaddady, P., Railkar, R. A., Musser, B. J., Cote, J., Ederveen,A. G.H., Krefetz,D. G., DeNoia,E., Free,A.L., Morrow, L., Chakravarthy, M. V., Kauh, E., Tatosian, D. A., and P.A. Kothare. (2017) Leveraging a clinical phase Ib proof-of-concept study for the GPR40 agonist MK-8666 in patients with type 2 diabetes for model informed phase II dose selection. Clin Transl Sci. 10, 404−411.

Li, N., Cui, Z., Fang, F., Lee, J.Y., and N. Ballatori. (2007). Heterodimerization, trafficking and membrane topology of the two proteins, Ost alpha and Ost beta, that constitute the organic solute and steroid transporter. Biochem J. 407, 363-372.

Mita, S., Suzuki, H., Akita, H., Hayashi, H., Onuki, R., Hofmann, A., and Y. Sugiyama. (2006). Inhibition of bile acid transport across Na+/taurocholate cotransporting polypeptide (SLC10A1) and bile salt export pump (ABCB 11)-coexpressing LLC-PK1 cells by cholestasis-inducing drugs. Drug Metab Dispos. 34:1575-81.

Monroe, J., Tanis, K., Podtelezhnikov, A., Nguyen, T., Mahotka, S., Lynch, D., Evers, R., Palamanda, J., Miller, R., Pippert, T., Cabalu, T., Johnson, T., Aslamkhan, A., Kang, W., Tamburino, A., Mitra, K., Agrawal, N., and F. Sistare. (2020). Application of a Rat Liver Drug Bioactivation Transcriptional Response Assay Early in Drug Development That Informs Chemically Reactive Metabolite Formation and Potential for Drug Induced Liver Injury. Toxicol Sci. Online ahead of print.

Moore, A., Chothe, P., Tsao, H., and N. Hariparsad. (2016). Evaluation of the Interplay between Uptake Transport and CYP3A4 Induction in Micropatterned Cocultured Hepatocytes. Drug Metab Dispos. 44:1910-1919.

Morgan, R., Van Staden, C., Chen, Y., Kalyanaraman, N., Kalanzi, J., Dunn, R., Afshari, C., and H. Hamadeh. (2013). A Multifactorial Approach to Hepatobiliary Transporter Assessment Enables Improved Therapeutic Compound Development. Toxicol Sci. 136:216-41.

N. Kaplowitz. (2001). Drug-induced liver disorders: implications for drug development and regulation. Drug Safety. 24, 483-490.

Pedersen, J.M., Matsson, P., Bergström, C.A., Hoogstraate, J., Norén, A., LeCluyse, E.L., and P. Artursson. (2013). Early identification of clinically relevant drug interactions with the human bile salt export pump (BSEP/ABCB11). Toxicol Sci. 136, 328-43.

Prueksaritanont, T., Chu, X., Evers, R., Klopfer, S. O., Caro, L., Kothare, P. A., Dempsey, C., Rasmussen, S., Houle, R., Chan, G., Cai, X., Valesky, R., Fraser, I.P., and S.A. Stoch. (2014). Pitavastatin is a more sensitive and selective organic anion-transporting polypeptide 1B clinical probe than rosuvastatin. Br. J. Clin. Pharmacol . 78, 587–598.

Rodrigues, A.D., Lai, Y., Cvijic, M.E., Elkin, L.L., Zvyaga, T., and M.G. Soars. (2014). Drug-induced perturbations of the bile acid pool, cholestasis, and hepatotoxicity: mechanistic considerations beyond the direct inhibition of the bile salt export pump. Drug Metab Dispos. 42, 566-74.

Shang, J., Tschirret-Guth, R., Cancilla, M., Samuel, K., Chen, Q., Chobanian, H.R., Thomas, A., Tong, W., Josien, H., Buevich, A.V., and K. Mitra. (2019). Bioactivation of GPR40 Agonist MK-8666: Formation of Protein Adducts in Vitro from Reactive Acyl Glucuronide and Acyl CoA Thioester. Chem Res Toxicol. Eprint.

Sistare, F.D., Mattes, W.B., and E.L. LeCluyse. (2016). The Promise of New Technologies to Reduce, Refine, or Replace Animal Use while Reducing Risks of Drug Induced Liver Injury in Pharmaceutical Development. ILAR J. 57, 186-211.

Swift, B., Pfeifer, N., and K. Brouwer. (2010). Sandwich–cultured hepatocytes: an in vitro model to evaluate hepatobiliary transporter–based drug interactions and hepatotoxicity. Drug Metab. Rev. 42: 446-471.

Ukairo, O., Kanchagar, C., Moore, A., Shi, J., Gaffney, J., Aoyama, S., Rose, K., Krzyzewski, S., McGeehan, J., Andersen, M.E., Khetani, S.R., and E.L. Lecluyse. (2013). Long-term stability of primary rat hepatocytes in micropatterned cocultures. J Biochem Mol Toxicol. 27, 204-12.

Wolf, K.K., Vora, S., Webster, L.O., Generaux, G.T., Polli, J.W., and K.L. Brouwer. (2010). Use of cassette dosing in sandwich-cultured rat and human hepatocytes to identify drugs that inhibit bile acid transport. Toxicol In Vitro. 24, 297-309.

Xu, Q., Liu, L., Vu, H., Kuhls, M., Aslamkhan, A.G., Liaw, A., Yu, Y., Kaczor, A., Ruth, M., Wei, C., Imredy, J., Lebron, J., Pearson, K., Gonzalez, R., Mitra, K., and F.D. Sistare. (2019). Can Galactose Be Converted to Glucose in HepG2 Cells? Improving the in Vitro Mitochondrial Toxicity Assay for the Assessment of Drug Induced Liver Injury. Chem. Res. Toxicol. 32, 1528-1544.

Yang, K., Guo, C., Woodhead. J.L., St Claire, R.L., Watkins, P.B., Siler, S.Q., Howell, B.A., and K.L.R Brouwer. (2016). Sandwich-Cultured Hepatocytes as a Tool to Study Drug Disposition and Drug-Induced Liver Injury. J Pharm Sci. 105, 443-59.

Yoshida, K., Maeda, K., and Y. Sugiyama. (2012). Transporter-mediated drug--drug interactions involving OATP substrates: predictions based on in vitro inhibition studies. Clin Pharmacol Ther. 91:1053-1064.

Yucha, R., He, K., Shi, Q., Cai, L., Nakashita, Y., Xia, C., and M. Liao. (2017). In Vitro Drug-Induced Liver Injury Prediction: Criteria Optimization of Efflux Transporter IC_{50} and Physicochemical Properties. Toxicol Sci. 157:487-499.

Zamek-Gliszczynski, M.J., Xiong, H., Patel, N.J., Turncliff, R.Z., Pollack, G.M., and K.L. Brouwer. (2003). Pharmacokinetics of 5 (and 6)-carboxy-2',7'-dichlorofluorescein and its diacetate promoiety in the liver. J Pharmacol Exp Ther. 304:801-809.

Zhang, Y., Jackson, J.P., St Claire, R.L., Freeman, K., Brouwer, K.R., and J.E. Edwards. (2017). Obeticholic acid, a selective farnesoid X receptor agonist, regulates bile acid homeostasis in sandwich-cultured human hepatocytes. Pharmacol Res Perspect. 5.

DMD Fast Forward. Published on September 17, 2020 as DOI: 10.1124/dmd.120.000086
This article has not been copyedited and formatted. The final version may differ from this version.

Footnote

This research was supported by Merck & Co., Inc., Kenilworth, NJ, USA and no external funding was received.

Figure Legends

Figure 1. The role of transporters in the entero-hepatic circulation of bile salts

Figure 2. The inhibitory effect of select inhibitors on the uptake of (A) TCA, (B) EA-SG, (C) $E_2$17βG, and (D) folic acid into membrane vesicles containing BSEP, MRP2, MRP3, and MRP4 in the presence or absence of ATP.

Figure 3. Establishment of an empirical BSEP cutoff based on a relationship between the estimated BSEP IC_{50} and liver $fu*I_{in,max}$. A) The estimated IC_{50} values for inhibition of BSEP-mediated TCA uptake into membrane vesicles in relation to the $fu*I_{in,max}$ for DILI negative and positive compounds with corresponding B) sensitivity analysis. The orange dotted line represents an empirical cutoff (based on eq. 2) where inhibition of BSEP may be predictive of human DILI for compounds that fall above the line. C) The estimated IC_{50} values for inhibition of BSEP-mediated TCA uptake into membrane vesicles in relation to DILI categorization. A cutoff of 5 uM yields similar specificity as that observed in panel A. (PPV = positive predictive value, NPV = negative predictive value)

Figure 4. The correlation between BSEP, MRP2, MRP3, and MRP4 inhibition and DILI risk. A) Heatmap of vesicular BSEP and MRP2 – 4 inhibition assay results for DILI negative and positive compounds. (red = above empirical cutoff for risk, green = below empirical cutoff for risk) B) Sensitivity analysis for vesicular MRP2-4 and BSEP + MRP2-4 inhibition assays.

Figure 5. Characterization studies show intact bile canaliculi and canalicular membrane localization of MRP2 and BSEP in MPCCs. A) Accumulation of CDF dye in bile canaliculi of MPCCs. B) Immunolocalization of MRP2 and BSEP in the canalicular membrane of MPCCs.

Figure 6. Accumulation of TCA into MPCCs. A) Time course of TCA accumulation into MPCCs and stromal cells in the presence of calcium. B) Uptake and efflux of TCA into MPCCs and stromal cells in the presence and absence of calcium at 10 min.

Figure 7. Inhibition of $Cl_{biliary}$ and BEI of TCA in MPCCs by CsA following a 10 min pretreatment. **A)** The inhibitory effect of CsA on the accumulation of 1 µM [^{3}H]TCA in the presence or absence of calcium in MPCCs. **B)** The inhibitory effect of CsA on $Cl_{biliary}$ in human MPCCs. **C)** The inhibitory effect of CsA on BEI in MPCCs. Results from a typical experiment are shown. Similar results were observed in 5 independent experiments.

DMD Fast Forward. Published on September 17, 2020 as DOI: 10.1124/dmd.120.000086
This article has not been copyedited and formatted. The final version may differ from this version.

Figure 8. Establishment of a cutoff in MPCCs to assess BSEP inhibition potential. A) IC_{50} values for the BEI of TCA in relation to the $fu*I_{in,max}$ for DILI negative and positive compounds. B) Correlation between BSEP vesicular and MPCC BEI inhibition assay results (red = assay positive, green = assay negative, gray = inconclusive due to solubility limitations). C) Corresponding sensitivity analysis for Panel A. The red dotted line in Panel A represents a 10 fold difference between $1/IC_{50}$ and $fu*I_{in,max}$. The black solid line represents cases were the IC_{50} was greater than the highest concentration tested. Since the IC_{50} is unknown, it cannot be compared to the $fu*I_{in,max}$ for compounds that fall to the right of the red dotted line and thus is not included in the sensitivity analysis in panel B.

Figure 9. Inhibition profile of MK-8666 and MK-8666 acyl glucuronide. A) MK-8666 inhibition of BSEP-mediated 1 µM [^{3}H]TCA uptake (% control) in membrane vesicles. B) The inhibitory effect of MK-8666 on BEI in MPCCs following a 24 hr preincubation. C) HR-MS analysis of MK-8666 MPCC samples following a 24 hr preincubation. D) MK-8666 acyl-glucuronide inhibition of BSEP-mediated 1 µM [^{3}H]TCA uptake (% control) in membrane vesicles.

Figure 10. Application of the vesicular BSEP and MPCC inhibition assays in lead optimization.

Table 1. Estimated IC_{50} values for BSEP and MRP2-4 generated in membrane vesicles for DILI negative and positive compounds. Corresponding unbound liver inlet concentrations were calculated from the highest clinical dose and associated C_{max}.

Compound	DILI Classification	Estimated IC_{50} (µM)				Dose (mg)	Cmax (µM)	fu	$fu*I_{in,max}$ (µM)
		BSEP	MRP2	MRP3	MRP4				
Ambrisentan	Negative	>100	>100	>100	>100	10	9.8	0.01	0.12
Amoxicillin	Negative	>100	>100	>100	>100	500	4.93	0.83	79.80
Amprenavir	Negative	98	>100	45.7	>100	1200	18	0.10	17.62
Aripiprazole	Negative	42.1	>100	>100	>100	15	0.13	0.01	0.02
Aspirin	Negative	>100	>100	45	>100	2000	77.7	0.004	3.27
Atorvastatin	Negative	6.3	>100	3.8	19.8	80	0.1	0.02	0.19
Buspirone	Negative	>100	>100	>100	>100	30	0.01	0.05	0.26
Caffeine	Negative	>100	>100	>100	>100	200	11.7	0.83	66.70
Carisoprodol	Negative	>100	>100	>100	>100	350	23	0.40	45.05
Cefprozil	Negative	38.2	>100	>100	>100	500	24.7	0.64	70.65
Cefuroxime	Negative	>100	33	>100	9	500	41.3	0.50	59.92
Chloramphenicol	Negative	>100	>100	>100	>100	666	10.3	0.47	69.27
Chlorpropamide	Negative	>100	>100	>100	>100	500	275	0.10	39.55
Cimetidine	Negative	>100	>100	>100	>100	1600	36.5	0.85	390.33
Ciprofloxacin	Negative	>100	>100	73	>100	600	9.66	0.80	104.30
Clarithromycin	Negative	>100	>100	71	34.9	500	5	0.41	20.32
Clofibrate	Negative	>100	>100	>100	>100	1000	404	0.08	54.30
Clotrimazole	Negative	10	>100	>100	>100	50	0.12	0.02	0.20
Diltiazem	Negative	>100	>100	>100	>100	500	0.3	0.30	24.21
Diphenhydramine	Negative	73	>100	>100	43	50	0.33	0.02	0.27
Dipyridamole	Negative	0.8	>100	>100	2.8	100	3.67	0.009	0.15
Disopyramide	Negative	>100	>100	>100	>100	800	22.4	0.50	89.75
Entacapone	Negative	11.4	52	9	0.7	200	3.28	0.02	0.94

Erythromycin	Negative	>100	>100	>100	>100	250	1.91	0.10	2.46
Esomeprasole	Negative	>100	>100	>100	>100	40	7	0.03	0.44
Famotidine	Negative	>100	>100	>100	>100	**160**	0.47	0.20	5.75
Fluoxetine	Negative	>100	43	32	>100	80	0.98	0.06	1.09
Furosemide	Negative	>100	>100	>100	1.7	480	32.7	0.02	2.07
Hydroxyzine	Negative	>100	>100	>100	>100	100	0.35	0.07	1.27
Levofloxacin	Negative	>100	>100	>100	>100	750	25.7	0.27	44.30
Lopinavir	Negative	7.4	>100	81	>100	800	18.8	0.02	2.07
Loracarbef	Negative	>100	>100	>100	>100	625	56.8	0.08	13.19
Megestrol	Negative	14.4	>100	>100	>100	800	2.73	0.02	3.39
Meloxicam	Negative	34	>100	>100	>100	15	9.1	0.01	0.07
Metformin	Negative	>100	>100	>100	>100	850	9.4	1.00	448.13
Nabumetone	Negative	>100	>100	>100	30.3	2000	315	0.01	8.99
Nadolol	Negative	84	>100	>100	>100	240	2.9	0.70	38.23
Naproxen	Negative	>100	>100	>100	25	500	423	0.01	5.68
Nifedipine	Negative	23	>100	>100	>100	30	0.26	0.08	0.48
Olanzapine	Negative	>100	>100	>100	>100	20	0.26	0.07	0.32
Omeprazole	Negative	22.5	>100	>100	>100	40	5.41	0.05	0.66
Paroxetine	Negative	>100	>100	59.5	>100	60	0.05	0.05	0.61
Pentoxyfilline	Negative	>100	>100	32.9	>100	400	0.3	0.30	28.87
Probenecid	Negative	68.5	>100	>100	>100	500	122	0.25	59.70
Propranolol	Negative	>100	>100	>100	>100	160	3.86	0.10	4.50
Quinidine	Negative	49.3	>100	>100	>100	400	4.84	0.20	17.43
Raloxifene	Negative	37	>100	>100	30.5	60	0	0.05	0.42
Ranitidine	Negative	>100	91	>100	>100	150	1.5	0.15	5.00
Rosiglitazone	Negative	0.6	>100	>100	4.3	8	1.4	0.002	0.01
Sumatriptan	Negative	>100	>100	>100	>100	200	0.2	0.86	39.12
Tacrine	Negative	>100	>100	>100	>100	160	0.17	0.45	24.29
Tetracycline	Negative	>100	>100	>100	>100	500	9	0.45	37.80
Tramadol	Negative	>100	>100	>100	>100	100	1.01	0.80	21.06

Trimethobenzamide	Negative	>100	>100	48.8	>100	300	10	1.00	61.49
Valsartan	Negative	16.2	>100	>100	>100	320	0.14	0.05	2.46
Verapamil	Negative	>100	>100	>100	52.7	120	0.6	0.10	1.82
Zolpidem	Negative	97	>100	56	>100	10	0.39	0.08	0.205
Acetaminophen	Positive	>100	>100	>100	>100	1000	64.6	0.90	455.04
Almorexant	Positive	1.7	>100	>100	>100	400	0.22	0.01	0.52
Alpidem	Positive	9.3	>100	>100	>100	50	0.07	0.01	0.05
Amiodarone	Positive	>100	>100	58	>100	600	0.7	0.04	2.51
Amoxicillin*-Clavulanate**	Positive	>100	>100	>100	40	300*/ 75**	9*/7.5**	0.88*/ 0.75**	56*/24**
Azithromycin	Positive	>100	>100	22.4	>100	2000	2.36	0.93	167.75
Benzbromarone	Positive	4.6	1.04	>100	1	300	42.4	0.01	0.90
Bosentan	Positive	37	>100	>100	22.2	125	2.54	0.02	0.35
Bromfenac	Positive	>100	>100	>100	1	50	12	0.001	0.02
Carbamazepine	Positive	>100	>100	>100	>100	200	11.6	0.24	16.33
Chlormezanone	Positive	>100	>100	>100	>100	600	32.9	0.52	93.09
Clopidogrel	Positive	36	>100	>100	>100	75	0.01	0.06	0.93
Clozapine	Positive	>100	>100	38	>100	300	3.67	0.03	1.95
Cyproterone Acetate	Positive	6.7	>100	>100	>100	100	0.53	0.04	0.66
Diclofenac	Positive	>100	>100	>100	30	100	0.84	0.01	0.23
Dilevalol	Positive	>100	>100	>100	>100	1200	1.12	0.50	122.40
Ethambutol	Positive	>100	>100	35	>100	2500	8.4	0.80	659.32
Felbamate	Positive	>100	>100	>100	>100	1200	192	0.78	411.68
Flucloxacillin	Positive	50.1	>100	>100	>100	250	16	0.05	2.64
Flutamide	Positive	>100	>100	>100	10.9	250	0.36	0.06	3.64
HCV-796	Positive	>100	>100	>100	>100	1000	4.93	0.48	73.26
Isoniazid	Positive	>100	>100	>100	>100	300	26.3	1.00	172.14
Labetalol	Positive	>100	>100	>100	>100	600	1.36	0.50	61.66
Lapatanib	Positive	1.2	>100	57.1	1.6	1250	2.12	0.01	0.92
Lumiracoxib	Positive	>100	>100	>100	9	400	25	0.02	2.32

Methimazole	Positive	56.1	>100	>100	>100	20	3.5	0.05	0.76
Methyldopa	Positive	>100	>100	>100	>100	500	10.4	0.90	151.40
Metiamide	Positive	>100	>100	100	>100				
MK-0377	Positive	>100	>100	30	>100				
MK-0536	Positive	>100	>100	>100	>100	400	9.9	0.01	0.71
MK-0571	Positive	1.2	8.58	17.2	0.4				
MK-0633	Positive	7.4	>100	>100	16.6	100	4	0.08	1.49
MK-0773	Positive	1.1	>100	>100	18.1	200	31.3	0.01	0.71
MK-0974	Positive	26.3	>100	>100	61.4	280	4	0.04	1.5
MK-A	Positive	>100	43	82	>100	400	0.6	0.26	12.26
MK-2461	Positive	4.1	48	>100	0.7	60	0.37	0.05	0.40
MK-2764	Positive	>100	>100	33	>100	600	0.93	0.14	10.20
MK-3207	Positive	0.5	>100	>100	>100	900	5	0.1	11.3
MK-3984	Positive	>100	>100	>100	>100	125	1.8	0.03	250.05
Nefazodone	Positive	2.8	>100	>100	>100	300	6.12	0.01	0.49
Nelfinavir	Positive	22.8	>100	>100	>100	250	5.3	0.02	0.69
Nevirapine	Positive	72	>100	>100	>100	200	5.81	0.40	22.31
Nitrofurantoin	Positive	>100	>100	>100	1.3	100	4.2	0.80	25.75
Nomifensine	Positive	>100	>100	>100	>100	200	18	0.40	29.58
Oxandrolone	Positive	>100	>100	67	>100	20	1.30	0.05	0.28
Panadiplon	Positive	>100	>100	>100	>100				
Pemoline	Positive	78	>100	55	>100	112	15.26	0.50	28.82
Perhexiline Maleate	Positive	>100	>100	30.2	>100	200	0.24	0.10	4.83
Ritonavir	Positive	0.7	85	31	25.5	600	15.3	0.02	1.42
Saquinavir	Positive	11	>100	23.9	>100	1000	8.25	0.02	2.15
Sitaxsentan	Positive	4.3	>100	>100	13.3	100	30.6	0.01	0.45
Sudoxicam	Positive	33	>100	>100	60				
Tasosartan	Positive	1.7	>100	>100	30.8	300	12.7	0.01	0.31
Telithromycin	Positive	4.2	>100	>100	>100	400	1.02	0.40	13.54
Ticlopidine	Positive	73	>100	>100	>100	250	3.8	0.02	1.34

Ticrynafen	Positive	41	>100	80.6	13	500	42.3	0.02	2.14
Tolcapone	Positive	12.1	46	>100	0.6	200	20.9	0.001	0.07
Troglitazone	Positive	1.3	6.3	>100	21.3	600	7.5	0.01	0.98
Trovafloxacin mesylate	Positive	>100	>100	>100	>100	200	5	0.30	11.11
Valproate	Positive	>100	>100	>100	>100	650	477	0.19	143.83
Verlukast	Positive	0.9	11.1	20.1	0.8	1500	241	0.001	0.44
Ximelagatran	Positive	>100	38	>100	>100				
Zafirlukast	Positive	4.5	11.5	>100	5.8	20	0.65	0.01	0.03
Zimelidine	Positive	>100	58.3	>100	>100	600	1.64	0.09	10.99

Table 2. IC_{50} values for $Cl_{biliary}$ and BEI of TCA generated in MPCCs for DILI negative and positive compounds. Bold values indicated values within 10 fold of the calculated $fu*I_{in,max}$. Met ID HR/MS data included as supplemental data.

Compound	DILI Classification	MPCCs				Vesicles BSEP IC_{50} (μM)	fu * $I_{in,max}$ (μM)	Met ID HR/MS Summary
		in vitro $Cl_{biliary}$ IC_{50} (μM)		BEI IC_{50} (μM)				
		10 min	24 hr	10 min	24 hr			
Ambrisantan	Negative	> 50	30.7 ± 14.1	> 50	23.6 ± 4	> 100	0.12	Parent ~23% 4 metabolites
Atorvastatin	Negative	> 50	12.9 ± 3.1	> 50	34.6 ± 4.8	6.3	0.19	Parent ~65% 5 metabolites
Buspirone	Negative	> 50	> 50	> 50	> 50	> 100	0.26	Parent 72% 5 metabolites
Dipyridamole	Negative	19.6 ± 7.8	19.5 ± 7.5	33.2 ± 14	> 25	0.8	0.15	Parent ~0% 1 metabolite
Entacapone	Negative	> 50	42.8 ± 8.9	> 50	> 50	11.4	0.94	Parent ~0% 4 metabolites
Lopinavir	Negative	**2.8 ± 0.6**	**3.2 ± 0.9**	**18.9 ± 3.5**	**9.8 ± 1.9**	7.4	2.07	Parent 78% 5 metabolites
Metformin	Negative	> 50	> 50	> 50	> 50	> 100	448.13	Parent ~100%
Pioglitazone*	Negative	4.9 ± 1.1	0.9 ± 0.3	24.8 ± 6.6	11.6 ± 3.4	< 1	0.13	Parent ~ 84% 11 metabolite
Quinidine	Negative	> 50	> 50	> 50	> 50	49.3	17.43	Parent ~87% 4 metabolites
Rosiglitazone	Negative	2.9 ± 1.8	2.6 ± 0.7	23.2 ± 8.1	> 50	0.6	0.01	Parent ~91% 1 metabolite
Valsartan	Negative	> 50	> 50	> 50	> 50	16.2	2.46	Parent ~100%

Acetaminophen	Positive	> 50	> 50	> 50	> 50	> 100	455.04	Parent ~97% 1 metabolite
Almorexant	Positive	53.3 ± 22.3	28.3 ± 17.6	> 50	> 50	1.7	0.52	Parent ~90% 8 metabolites
Benzbromarone	Positive	**3.7 ± 0.7**	**2.5 ± 1.1**	31.7 ± 7.9	**5.4 ± 1**	4.6	0.9	Parent ~90% 3 metabolites
Bosentan	Positive	38.3 ± 9.5	10.9 ± 2.7	> 50	37 ± 5.9	37	0.35	Parent ~87% 4 metabolites
Cyclosporin A	Positive	**2.4 ± 0.8**	**1.1 ± 0.2**	**4.7 ± 1.3**	**2.2 ± 0.4**	0.3	4.7	Parent ~95% 3 metabolites
Cyproterone Acetate	Positive	26.5 ± 7.9	17.6 ± 8.6	> 50	> 50	6.7	0.66	Parent 59% 3 metabolites
Lapatanib	Positive	> 25	> 25	> 25	> 25	1.2	0.92	Parent ~61% 3 metabolites
MK-0773	Positive	27.2 ± 11.2	15.5 ± 2.3	> 50	> 50	1.1	0.71	Parent ~88% 4 metabolites
MK-0974	Positive	15.3 ± 5	**11.7 ± 5**	46 ± 17.6	16 ± 8.1	26.3	1.5	Parent ~96% 3 metabolites
MK-3207	Positive	43 ± 9.9	> 50	> 50	> 50	0.5	11.3	Parent ~91% 2 metabolites
Nefazodone	Positive	> 50	30.9 ± 9.3	> 50	> 50	2.8	0.49	Parent ~80% 6 metabolites
Ritonavir	Positive	**6.9 ± 2.4**	**4.1 ± 1.6**	38.5 ± 7.6	**6.9 ± 2.1**	0.7	1.42	Parent 99% 1 metabolite
Sitaxsentan	Positive	6.5 ± 2.1	**3.3 ± 0.9**	> 50	11.9 ± 2.2	4.3	0.45	Parent ~99% 1 metabolite
Tasosartan	Positive	44.3 ± 16.2	9.7 ± 2.9	> 50	39 ± 8.4	1.7	0.31	Parent ~75% 6 metabolites
Telithromycin	Positive	**39.6 ± 17.2**	**21.7 ± 11.7**	> 50	**39.8 ± 7.7**	4.2	13.54	Parent ~79% 4 metabolites
Tolcapone	Positive	20.2 ± 6.4	14.5 ± 2	> 50	> 50	12.1	0.07	Parent ~4% 2 metabolites

Troglitazone	Positive	**2.2 ± 0.3**	**0.8 ± 0.2**	14.3 ± 2.9	**8.5 ± 1.7**	1.3	0.98	Parent ~1% 6 metabolites
Verlukast	Positive	15.2 ±3.5	12.1 ± 2.9	> 50	> 50	0.9	0.44	Parent ~87% 3 metabolites
Zafirlukast	Positive	11.7 ± 4.5	3 ± 0.7	> 50	8.4 ± 1.5	4.5	0.03	Parent ~71% 3 metabolites

* Pioglitazone was not included in original test set. Pioglitazone $fu^*I_{in,max}$ based on a dose of 45 mgs with corresponding C_{max} of 4.2 µM and an unbound fraction of 0.01.

DMD Fast Forward. Published on September 17, 2020 as DOI: 10.1124/dmd.120.000086
This article has not been copyedited and formatted. The final version may differ from this version.

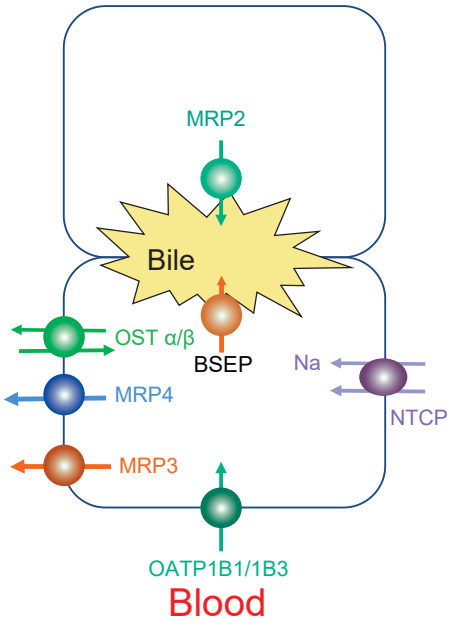

Figure 1

DMD Fast Forward. Published on September 17, 2020 as DOI: 10.1124/dmd.120.000086
This article has not been copyedited and formatted. The final version may differ from this version.

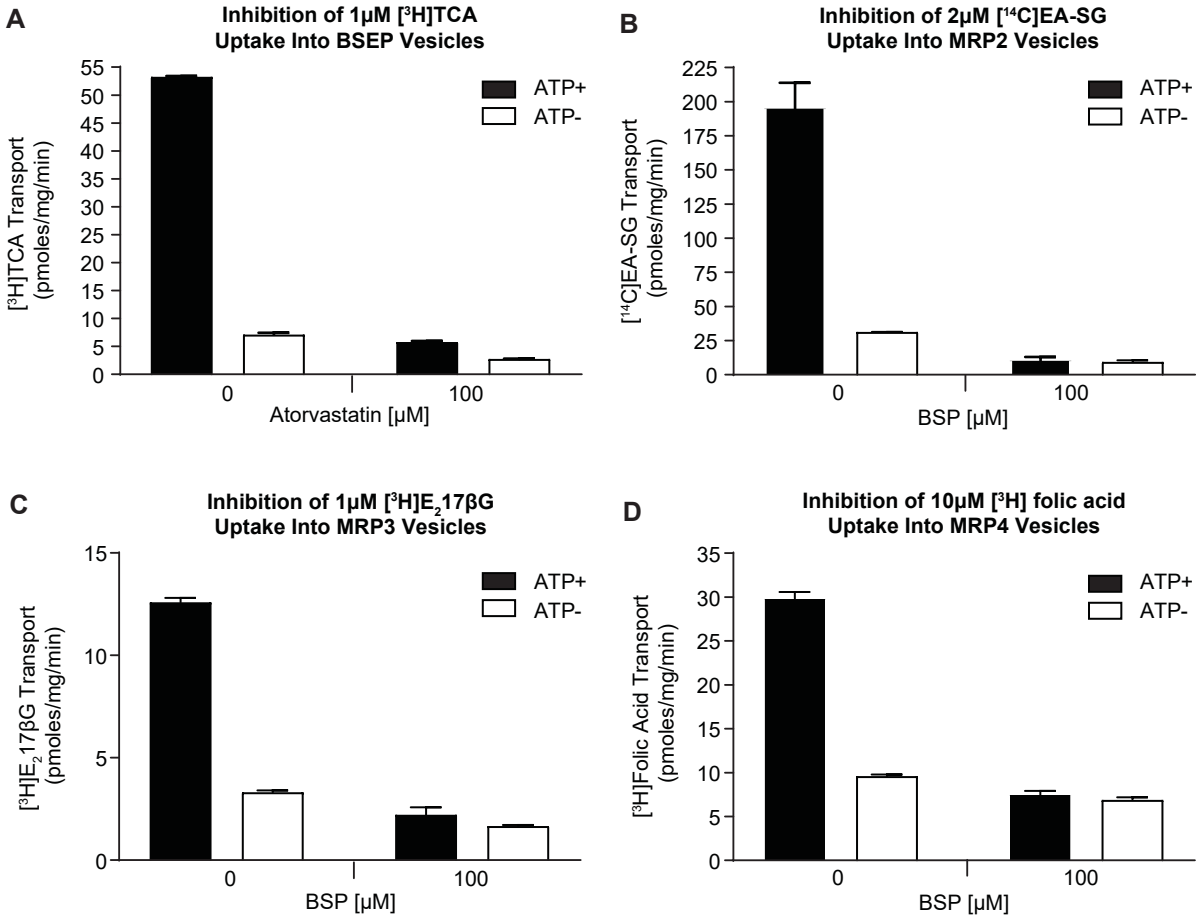

Figure 2

DMD Fast Forward. Published on September 17, 2020 as DOI: 10.1124/dmd.120.000086
This article has not been copyedited and formatted. The final version may differ from this version.

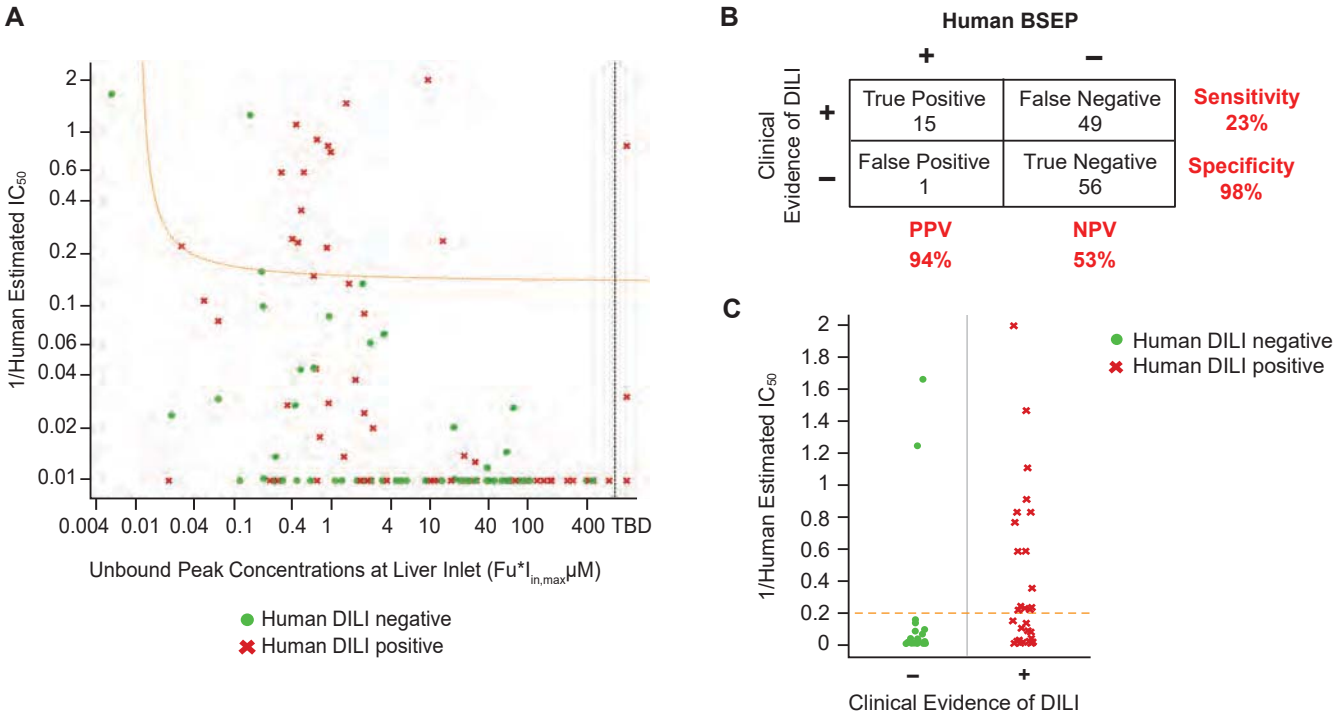

Figure 3

DMD Fast Forward. Published on September 17, 2020 as DOI: 10.1124/dmd.120.000086
This article has not been copyedited and formatted. The final version may differ from this version.

A

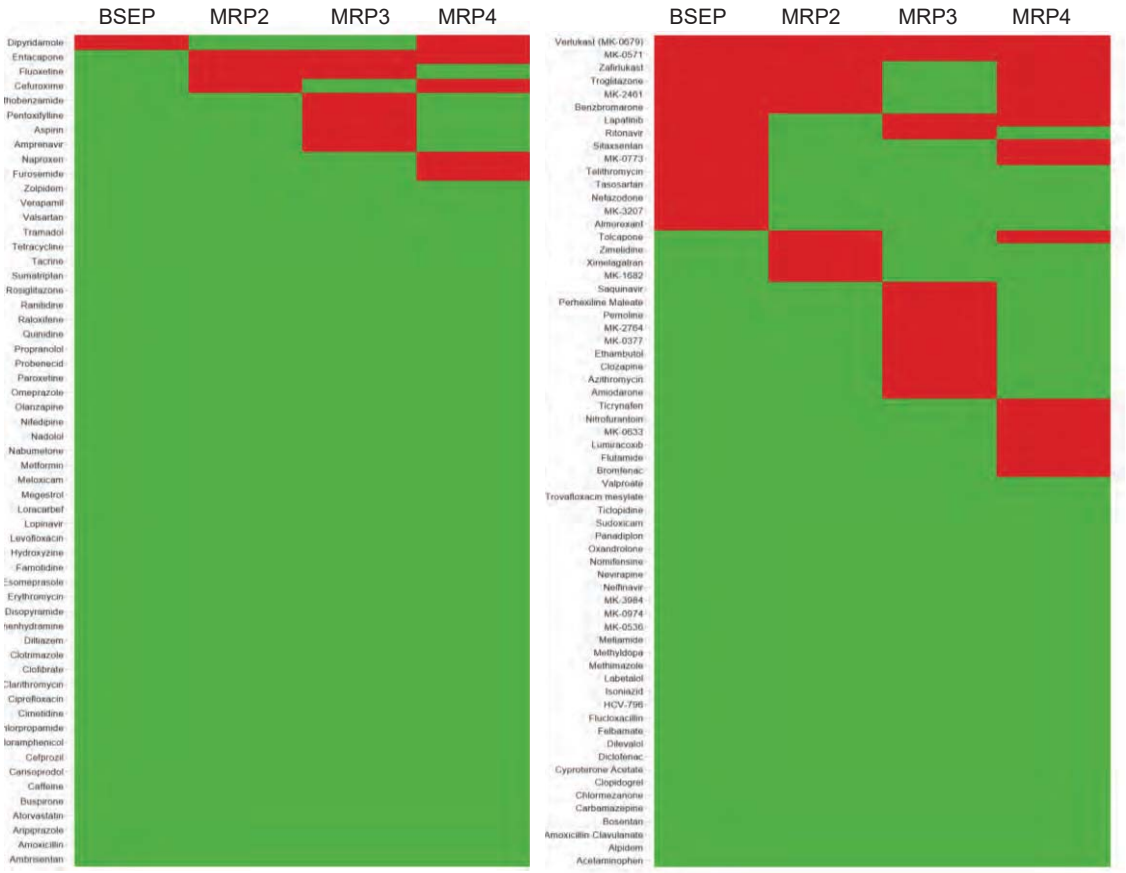

B

Human MRP2

Clinical Evidence of DILI	+	–	
+	True Positive 10	False Negative 54	Sensitivity 15%
–	False Positive 3	True Negative 54	Specificity 95%
	PPV 77%	NPV 50%	

Human MRP3

Clinical Evidence of DILI	+	–	
+	True Positive 13	False Negative 51	Sensitivity 20%
–	False Positive 6	True Negative 51	Specificity 89%
	PPV 68%	NPV 50%	

Human MRP4

Clinical Evidence of DILI	+	–	
+	True Positive 16	False Negative 48	Sensitivity 25%
–	False Positive 5	True Negative 52	Specificity 91%
	PPV 76%	NPV 52%	

Human BSEP or MRP2

Clinical Evidence of DILI	+	–	
+	True Positive 19	False Negative 45	Sensitivity 30%
–	False Positive 4	True Negative 53	Specificity 93%
	PPV 83%	NPV 54%	

Human BSEP or MRP3

Clinical Evidence of DILI	+	–	
+	True Positive 24	False Negative 40	Sensitivity 38%
–	False Positive 7	True Negative 50	Specificity 88%
	PPV 77%	NPV 56%	

Human BSEP or MRP4

Clinical Evidence of DILI	+	–	
+	True Positive 22	False Negative 42	Sensitivity 34%
–	False Positive 5	True Negative 52	Specificity 91
	PPV 81%	NPV 55%	

Human BSEP, MRP2, MRP3, or MRP4

Clinical Evidence of DILI	+	–	
+	True Positive 34	False Negative 30	Sensitivity 53%
–	False Positive 10	True Negative 47	Specificity 82%
	PPV 77%	NPV 61%	

Figure 4

DMD Fast Forward. Published on September 17, 2020 as DOI: 10.1124/dmd.120.000086
This article has not been copyedited and formatted. The final version may differ from this version.

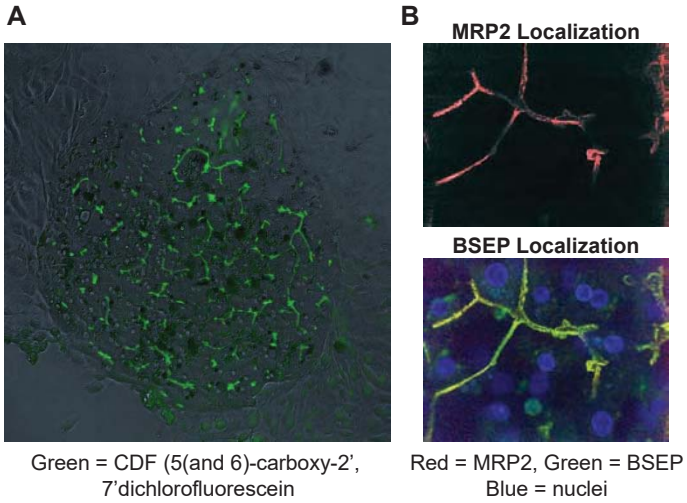

Figure 5

DMD Fast Forward. Published on September 17, 2020 as DOI: 10.1124/dmd.120.000086
This article has not been copyedited and formatted. The final version may differ from this version.

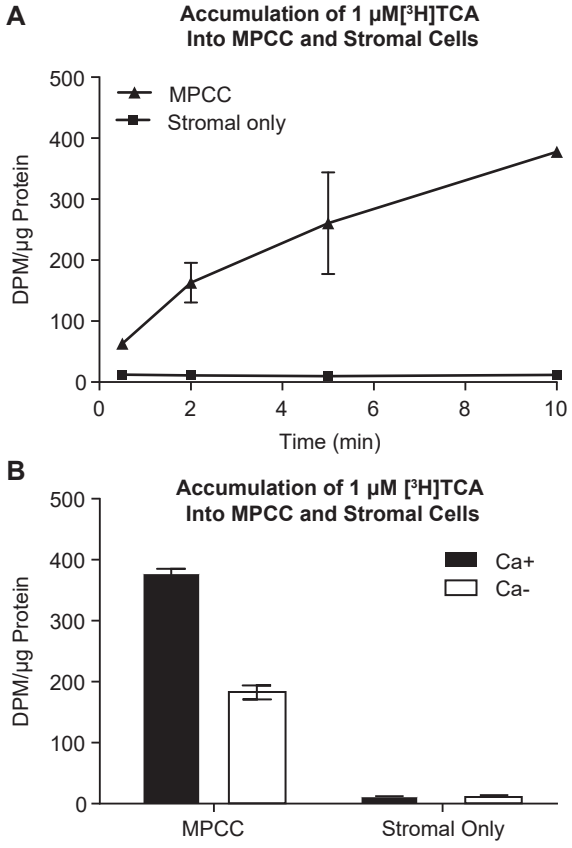

Figure 6

DMD Fast Forward. Published on September 17, 2020 as DOI: 10.1124/dmd.120.000086
This article has not been copyedited and formatted. The final version may differ from this version.

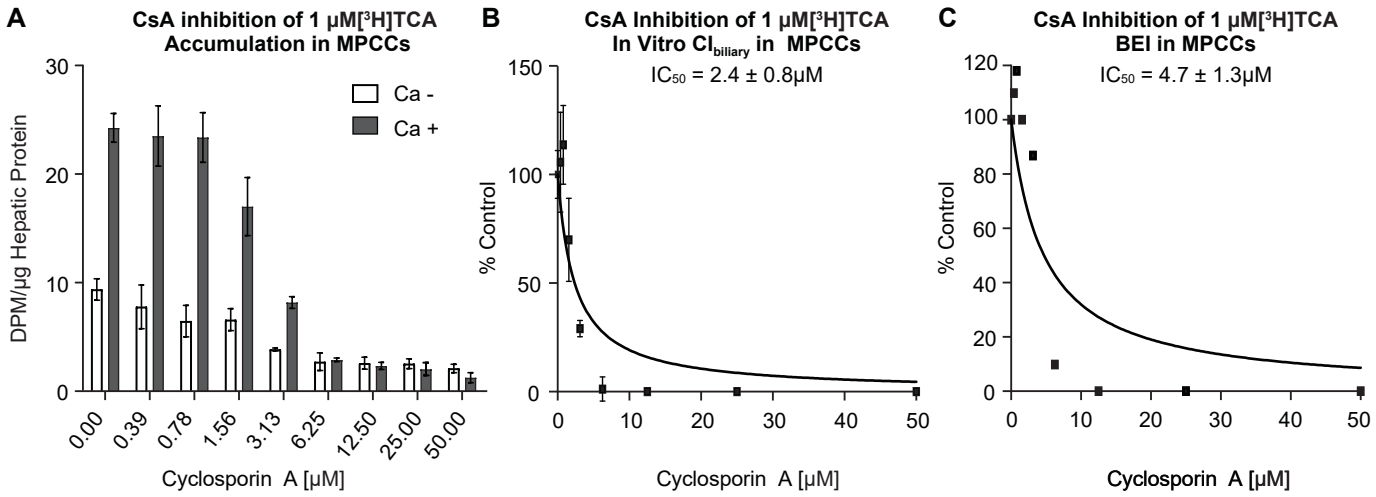

Figure 7

DMD Fast Forward. Published on September 17, 2020 as DOI: 10.1124/dmd.120.000086
This article has not been copyedited and formatted. The final version may differ from this version.

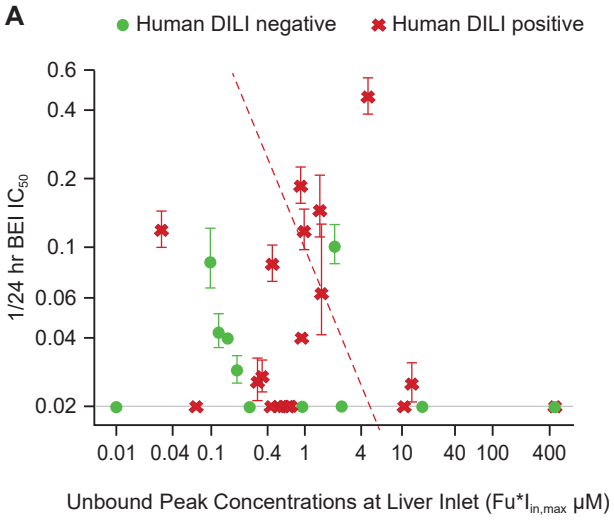

B

DILI Negative

Compound	BSEP Vesicular Inhibition	MPCC BEI Inhibition
Dipyridamole		
Lopinavir		
Ambrisantan		
Atorvastatin		
Buspirone		
Entacapone		
Pioglitazone		
Rosiglitazone		
Valsartan		
Metformin		
Quinidine		

DILI Positive

Compound	BSEP Vesicular Inhibition	MPCC BEI Inhibition
Benzbromarone		
Cyclosporine A		
Ritonavir		
Telithromycin		
Troglitazone		
Almorexant		
Lapatanib		
MK-0773		
Nefazodone		
Sitaxsentan		
Tasosartan		
Verlukast		
Zafirflukast		
MK-3207		
Bosentan		
Cyproterone		
MK-0974		
Tolcapone		
Acetaminophen		

C

1/BEI IC_{50} <10x $fu^*I_{in,max}$

Clinical Evidence of DILI	+	−	
+	True Positive 5	False Negative 12	Sensitivity 29%
−	False Positive 1	True Negative 8	Specificity 89%
	PPV 83%	NPV 40%	

Figure 8

DMD Fast Forward. Published on September 17, 2020 as DOI: 10.1124/dmd.120.000086
This article has not been copyedited and formatted. The final version may differ from this version.

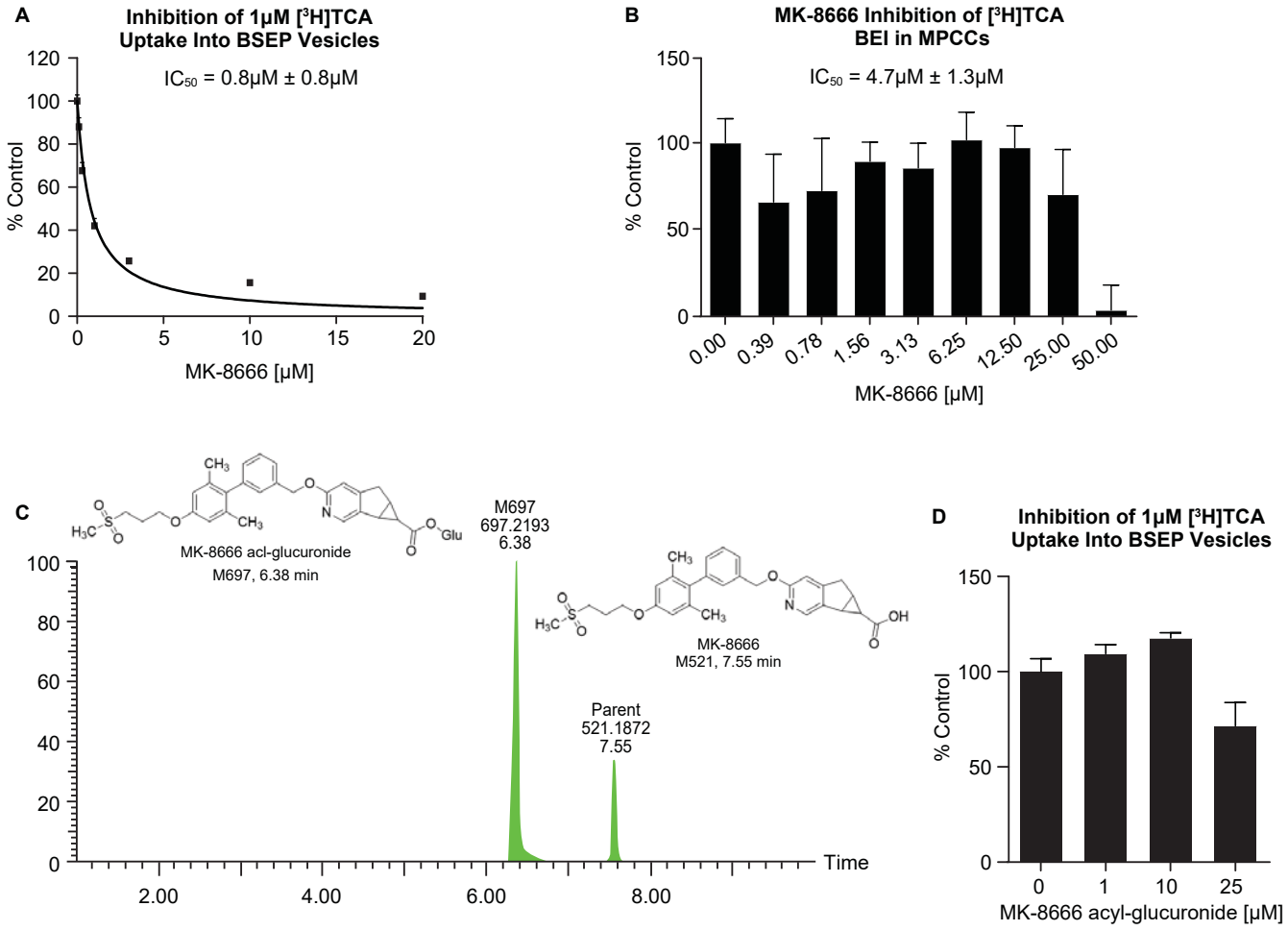

Figure 9

DMD Fast Forward. Published on September 17, 2020 as DOI: 10.1124/dmd.120.000086
This article has not been copyedited and formatted. The final version may differ from this version.

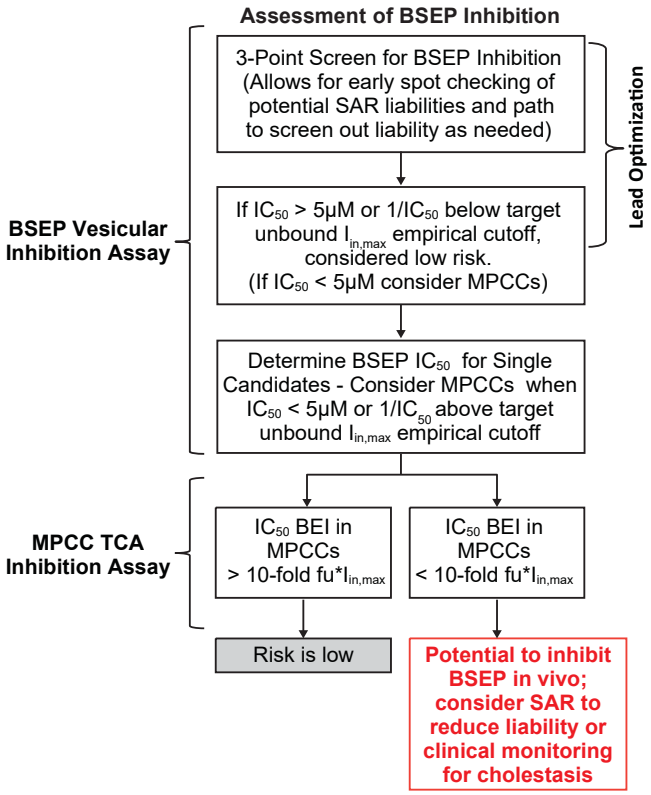

Figure 10